now believed that the activity of SFK is determined by an equilibrium between an inactive (phosphorylated) and a primed (dephosphorylated) state regulated by a balance of Csk and its counteracting tyrosine phosphatase(s). Upon cell stimulation, SFKs at a primed state become functionally activated to relay signals into the cells. Thus, perturbation of the equilibrium status of SFK, potentially induced by up- or downregulation of Csk and/or a tyrosine phosphatase(s) during development and/or cancer progression, may greatly affect the sensitivity of the cells to extracellular cues. In relation to cancer progression, it has been reported that c-Src-induced transformation of cells bearing v-Crk was suppressed by Csk overexpression (Sabe *et al.*, 1992b). In addition, downregulation of Src kinase activity by adenovirus-mediated csk gene transfer has been shown to abrogate the metastatic phenotype of colon cancer cells (Nakagawa *et al.*, 2000). We previously reported a reduction of Csk protein in about 60% of human colon cancer cases in which there was an elevation of Src activity, indicating that reduction of Csk may be one of the causes of the elevated specific activity of c-Src (Rengifo-Cam *et al.*, 2001). These findings suggest that Csk could be involved in the regulation of some cancer progression, through controlling the activity status of multiple SFKs. However, the precise function of Csk in human colon cancer cells has not been yet established. To address this issue, we examined the effects of modulation of Csk function on the phenotypes of human colon cancer cells. We here show that the equilibrium status of SFK controlled by Csk could control the integrin-mediated cell adhesion and migration implicated in the metastatic potential of human colon cancer cells.

Results and discussion

Expression and activity of SFK in human epithelial colon cancer cells

We first analysed protein expressions of Csk and SFK and the activity status of SFK in human colon cancer cell lines (Dan *et al.*, 2002), HCC2998, HCT15 and HT29 (Figure 1a). Consistent with previous observations (Rosen *et al.*, 1986; Rengifo-Cam *et al.*, 2001), HCT15 and HT29 cells showed substantial elevation of c-Src expression and a reduced expression of Csk compared with HCC2998 cells, a highly differentiated adenocarcinoma cell line (Kobayashi *et al.*, 1999). It was also shown that all these cells express multiple members of SFK including Yes, Fyn, Lyn and Lck, although there were no dramatic changes in their expressions among them. The activity status of SFK was then assessed with anti-Src pY418 antibody that can recognize autophosphorylated tyrosines of SFKs (SFK pY418), since SFK autophosphorylation is directly associated with its function (Sabe *et al.*, 1992a, b). HCC2998 cells demonstrated only faint signals for SFK autophosphorylation, while HCT15 and HT29 cells showed substantial phosphorylation on SFKs potentially corresponding to c-Src and c-Yes. In contrast, phosphorylations at the negative regulatory sites, Y529,

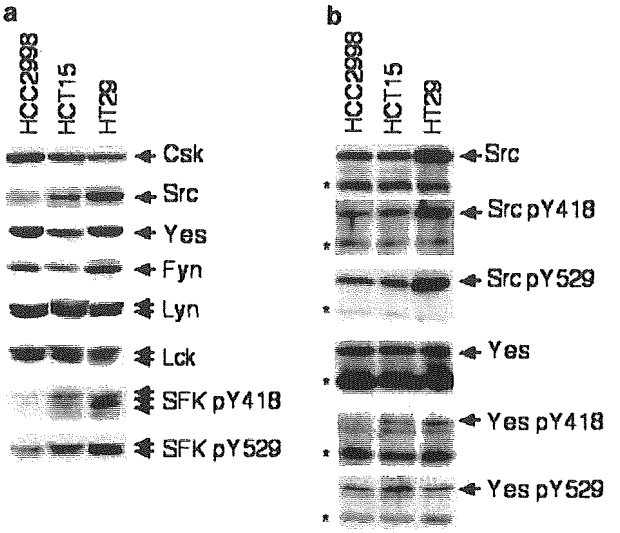

Figure 1 Expression and phosphorylation status of SFK in human colon cancer cells. (**a**) Total cell lysates from HCC2998, HCT15 and HT29 cells were obtained using ODG buffer, and equal amounts (20 μg protein) were analysed by Western blotting using specific antibodies against the indicated proteins. Anti-Src pY418 and pY529 detected multiple members of phosphorylated SFKs indicated by arrows. (**b**) c-Src and c-Yes proteins were immunoprecipitated using total lysate (500 μg protein) from the cancer cells, and probed with anti-Src, anti-Yes, anti-Src pY418 and anti-Src pY529 antibodies. Asterisks indicate the bands of immunoglobulin heavy chain

were steadily detected in all cell types with the highest levels in HT29 cells. To verify the phosphorylation levels of individual SFK members, c-Src and c-Yes proteins were immunoprecipitated and subjected to Western blotting (Figure 1b). In HT29 cells, c-Src was substantially phosphorylated at both Y418 and Y529, revealing that some c-Src are at primed state, while others are downregulated by Csk. In the case of c-Yes, phosphorylation at Y418 was the most evident in HT29 cells, while Y529 appeared to be less phosphorylated in the same cell line. These observations demonstrate that not only c-Src but also some other SFKs including c-Yes are basally primed in advanced cancer cells such as HT29, but only slightly activated in highly differentiated HCC2998 cells. This raises the possibility that perturbation of the balance between SFK and Csk, potentially achieved by elevated expression of SFK, downregulation of Csk or both, might influence the activity status of SFK in cancer cells. In order to address the role of such regulatory system of SFK in cancer progression, we here modulated the SFK–Csk balance by introducing Csk into HCT15 and HT29 cells, and observed its effects on the activity status of SFK and the phenotypic features of cancer cells.

Modulation of SFK by Csk influences cell morphology, cell–cell interaction, cell motility and in vitro *invasiveness in colon cancer cells*

We introduced wild-type Csk (Csk K+) or kinase-negative mutant of Csk (Csk K−) in HCT15 and HT29

cells using an adenovirus expression system (Takayama *et al*., 1999). Adenovirus infection readily induced protein expression in almost 100% of the cells, and did not affect the viability or growth rate of the cells (data not shown). The expression of Csk K+ suppressed the autophosphorylation of SFK (pY418) while that of Csk K− enhanced it (Figure 2a), demonstrating that Csk K+ suppressed the activity of SFK and Csk K− acted dominant negatively in inducing the activation of SFK. The effect of Csk overexpression on the morphologies of HCT15 and HT29 cells were observed by phase contrast microscopy (Figure 2b). Overexpression of Csk K+ in either cell types induced a dramatic change in cell morphology; the majority of cells formed compact cell aggregates (Figure 2bB and G). On the other hand, cells expressing Csk K− (Csk K− cells) appeared scattered and exhibited a mesenchymal-like phenotype, although HT29

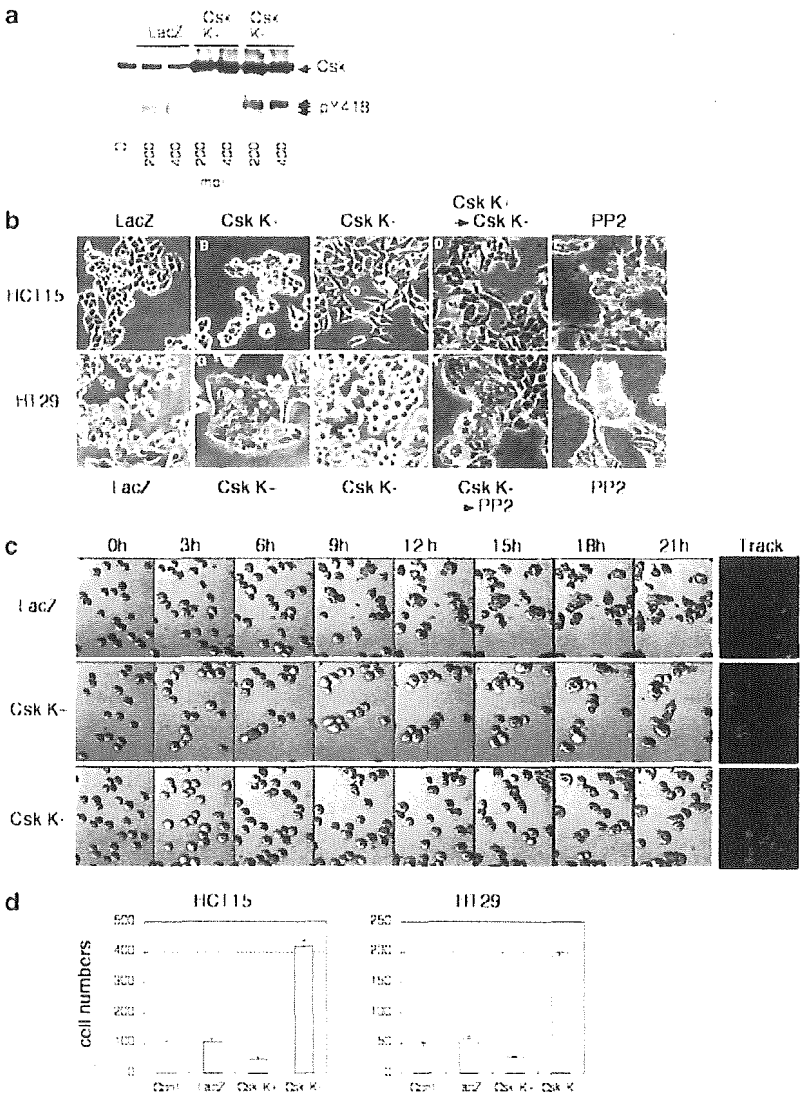

Figure 2 Effect of adenovirus-mediated overexpression of Csk on cell morphology, cell–cell interaction, cell motility and *in vitro* invasiveness in colon cancer cells. (**a**) Expression of Csk protein induced by adenovirus-mediated gene transfer. HCT15 cells were infected with indicated m.o.i. of adenoviruses carrying LacZ, wild-type Csk (Csk K+) and kinase-negative mutant Csk (Csk K−), and the total cell lysates were subjected to Western blotting with anti-Csk (upper panel) and anti-Src pY418 (lower panel) antibodies. Location of Csk and phosphorylated SFKs are indicated by arrows. (**b**) Phase-contrast pictures were taken from HCT15 and HT29 cells after 48 h treatment with LacZ (A and F), Csk K+ (B and G) or Csk K− (C and H), respectively. HCT15 cells treated with Csk K+ were subjected to secondary treatment with Csk K− (D). HCT15 cells were incubated with 10 μM PP2 for 24 h (E). HT29 cells treated with (I) or without (J) Csk K− were incubated with 10 μM PP2 for 24 h. (**c**) HT29 cells infected with indicated viruses for 24 h were replated, and their cell movements was monitored for 21 h by time-laps video microscopy. Images at 3 h intervals are shown. In each cell type, five cells were arbitrarily selected and tracked to assess the ability of cell motility using Move-tr/2D software (right panels). (**d**) *In vitro* invasiveness of HCT15 and HT29 cells without virus infection (control) or those infected with virus carrying LacZ, Csk K+ and Csk K−. Cells (1.0×10^5) were seeded into matrigel invasion chambers. After 48 h, membranes were detached and cells were stained and counted under light microscopy. Results are expressed as mean values of three experiments

cells still exhibited round shape (C and H). When the aggregated HCT15 cells expressing Csk K+ were subsequently infected with virus carrying Csk K−, the cells became scattered again, demonstrating that the morphological changes can be regulated reversibly (D). As reported previously (Nam *et al*., 2002), treatment with PP2, a specific inhibitor of SFK, induces cell aggregation in both cell types (E and J). Cell aggregation could also be induced by the PP2 treatment in HT29 cells expressing Csk K− (I). The morphology of PP2-treated cells is somewhat similar to that of Csk K+ cells, supporting the idea that morphological changes induced by Csk expression are mediated by the modulation of SFK activity.

To further characterize Csk-expressing cancer cells, the infected HT29 cells were replated onto collagen-coated dishes and their behaviors were observed for 21 h under time-laps video microscopy. The images at 3 h intervals and the tracks of five cells in each cell type are shown in Figure 2c. Overexpression of Csk K+ appeared to attenuate cell motility, and also the cells tended to associate with each other resulting in the formation of compact cell aggregates. In contrast, the Csk K− cells actively migrated without forming the cell aggregates. We then assessed the *in vitro* invasive potential of the infected HCT15 and HT29 cells by matrigel assay (Figure 2d). The Csk K− cells efficiently invaded matrigel, whereas the invasiveness of Csk K+ cells was rather suppressed. This supports the previous observation showing that adenovirus-mediated csk gene transfer can abrogate the metastatic phenotype of colon cancer cells *in vivo* (Nakagawa *et al*., 2000). Taken together, these observations suggest that the activity status of SFK regulated by Csk might influence the ability of cell migration implicated in the metastatic potential of human colon cancer (Avizienyte *et al*., 2002).

Modulation of SFK by Csk influences integrin-SFK-mediated cell adhesion signaling

We then addressed the molecular mechanisms that determine the phenotypes of the infected HT29 cells. When cells were plated onto culture dishes coated with collagen I, evident changes in morphology were observed again; overexpression of Csk K+ induced formation of large cell aggregates, while that of Csk K− facilitated the cell scattering and destabilized cell–cell contacts (Figure 3aA–C). However, when cells were plated onto laminin-coated dishes, the morphological change became more moderate and large cell aggregates were stably formed even in Csk K− cells (Figure 3aD–F). These findings suggest that the effects of Csk are dependent on cell adhesion mediated by specific integrins that can respond to collagen I. To confirm this, cell adhesion assay on collagen I was performed. As shown in Figure 3b, cell adhesion was apparently suppressed by the expression of Csk K+, while it was greatly enhanced by that of Csk K−. The changes in tyrosine phosphorylation of cellular proteins during cell adhesion process were then examined by Western blotting (Figure 3c). In suspended cells, SFK is phosphorylated dominantly at Y529 in Csk K+ cells, while in Csk K− cells, it is phosphorylated at Y418. This can be attributed to a change in the equilibrium of SFK to an inactive state in Csk K+ cells and to a primed state in Csk K− cells. Upon cell adhesion, the primed SFK in Csk K− cells became functionally activated resulting in a dramatic increase in tyrosine phosphorylation of several SFK targets including FAK and paxillin, which play crucial roles in the formation of focal contacts. Phosphorylation of FAK Y397 was also induced, reflecting the activation of FAK implicated in the regulation of cell migration and invasion (Hauck *et al*., 2002). In contrast, inactive state of SFK in Csk K+ cells cannot be activated through integrin signaling, and consequently there is no significant increase in the phosphorylation of cell adhesion-related proteins. The importance of cell adhesion mediated by specific integrin was further supported by the observation that tyrosine phosphorylation of cell adhesion proteins was not induced even in Csk K− cells when plated onto laminin or poly- D-lysine-coated dishes (data not shown). These results show that Csk is critical to define the sensitivity of the cells to the integrin-SFK-mediated cell adhesion signaling.

Modulation of SFK by Csk influences focal contact formation and actin cytoskeletal organization

We next investigated the cellular localizations of tyrosine phosphorylated proteins (pY), vinculin, as markers of focal contact, and actin fiber (F-actin) by confocal microscopy (Figure 4a). Csk K+ cells showed reduced numbers of staining patches of pY and vinculin that were localized only at the edge of large cell aggregates, suggesting that focal contacts are formed at places that can directly interact with the substrate (Figure 4a and c, B). Consistent with this, staining of F-actin was evident only at the edge of cell aggregates as well (Figure 4a and c, E). In contrast, in Csk K− cells, the number of focal contacts was greatly increased, and they appeared surrounding the individual cells (Figure 4a and c, C). F-actin was also enriched around the focal contacts of each cell (Figure 4a and c, F). At the middle surface of Csk K+ cells, F-actin appeared highly concentrated at cell–cell contacts probably for the support of E-cadherin/β-catenin complex (Figure b, E), whereas in Csk K− cells, such actin support was substantially reduced (Figure b, F). These observations indicate that expression of Csk K+ suppresses the formation of focal contacts while that of Csk K− enhances it through the increased phosphorylation of cell adhesion machinery, and that there is a drastic rearrangement of actin cytoskeletal organization accompanied by the formation of focal contacts.

Modulation of SFK by Csk does not affect the E-cadherin/β-catenin complex

We here addressed the mechanism by which cell–cell contact is stabilized in Csk K+ cells, while it is

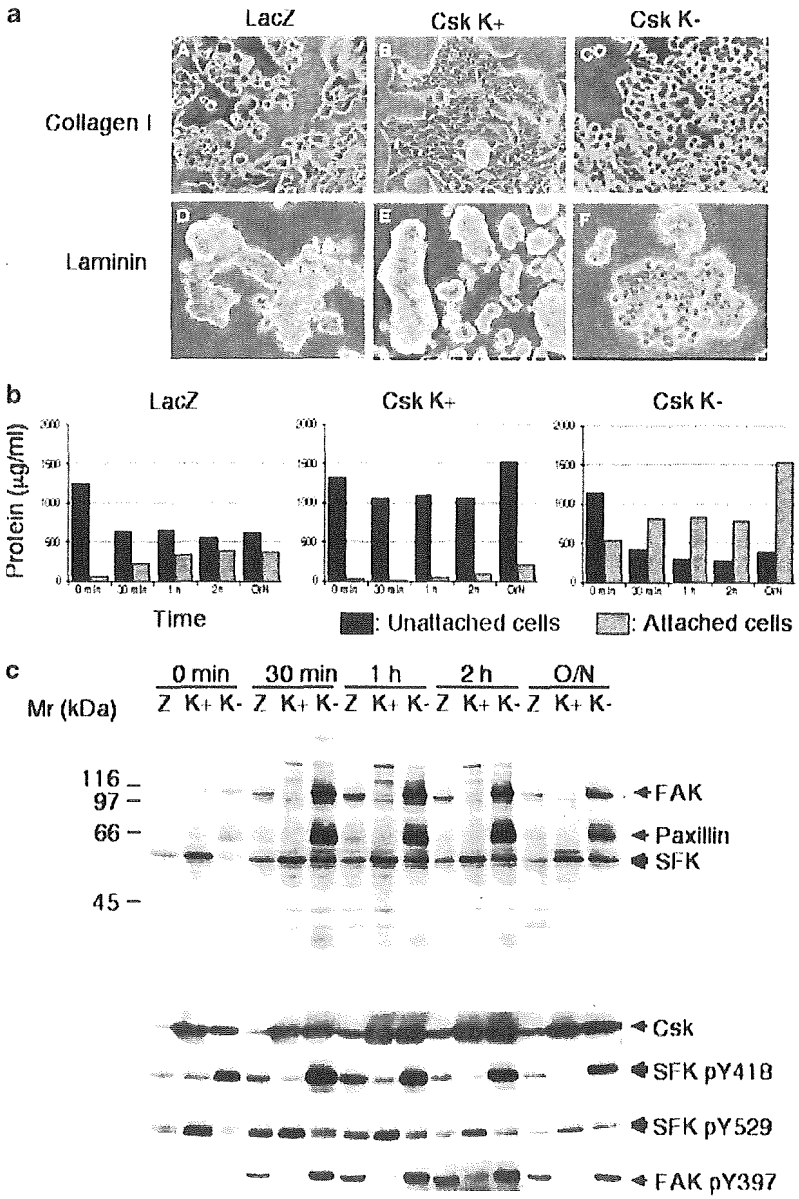

Figure 3 Effect of Csk overexpression on cell adhesion signaling in HT29 cells. (**a**) Phase-contrast pictures of HT29 cells infected with adenovirus carrying LacZ (A and D), Csk K + (B and E) or Csk K− (C and F). Cells were seeded onto plastic slides coated with collagen I (A, B and C) or plastic slides coated with laminin (D, E and F). (**b**) Cell adhesion assay on collagen I. HT29 cells infected with adenovirus carrying LacZ, Csk K + or Csk K− were once detached and replated onto collagen I-coated dishes. After indicated periods, adherent and nonadherent cells were separately collected and the amounts of cellular proteins were determined. Here '0 min' means the minimum period taken between replating and cell harvesting. Protein amounts of nonadherent and adherent cells are indicated by black and gray bars, respectively. (**c**) Changes in tyrosine phosphorylation in response to cell adhesion. After replating the infected HT29 cells onto collagen I-coated dishes for indicated periods, total cell lysates were obtained, and total tyrosine phosphorylation level (upper panel) and expression of Csk and tyrosine phosphorylation of Src Y418, Src Y529, FAK Y397 (lower panels) were analysed by Western blotting. Z; cells expressing LacZ, K +; Csk K + cells, K−; Csk K− cells

destabilized in Csk K− cells. It is known that E-cadherin plays a major role in cell–cell contact of epithelial cells (Hyafil *et al*., 1980). Indeed, an anti-E-cadherin antibody could completely inhibit the formation of compact cell aggregates in Csk K + cells (Figure 5a), suggesting that SFK activity under the control of Csk is involved in the regulation of E-cadherin-mediated cell–cell contacts. Previous reports have suggested a role for activated form of Src in dissociating the E-cadherin/β-catenin complex (Irby and Yeatman, 2002). Thus, we investigated the localization of E-cadherin and its partner β-catenin in HT29 cells expressing Csk K + or Csk K−. However, there was no apparent difference in the staining patterns of either E-cadherin or β-catenin in any type of cells (Figure 5b). Both E-cadherin and β-catenin were predominantly localized at the membrane

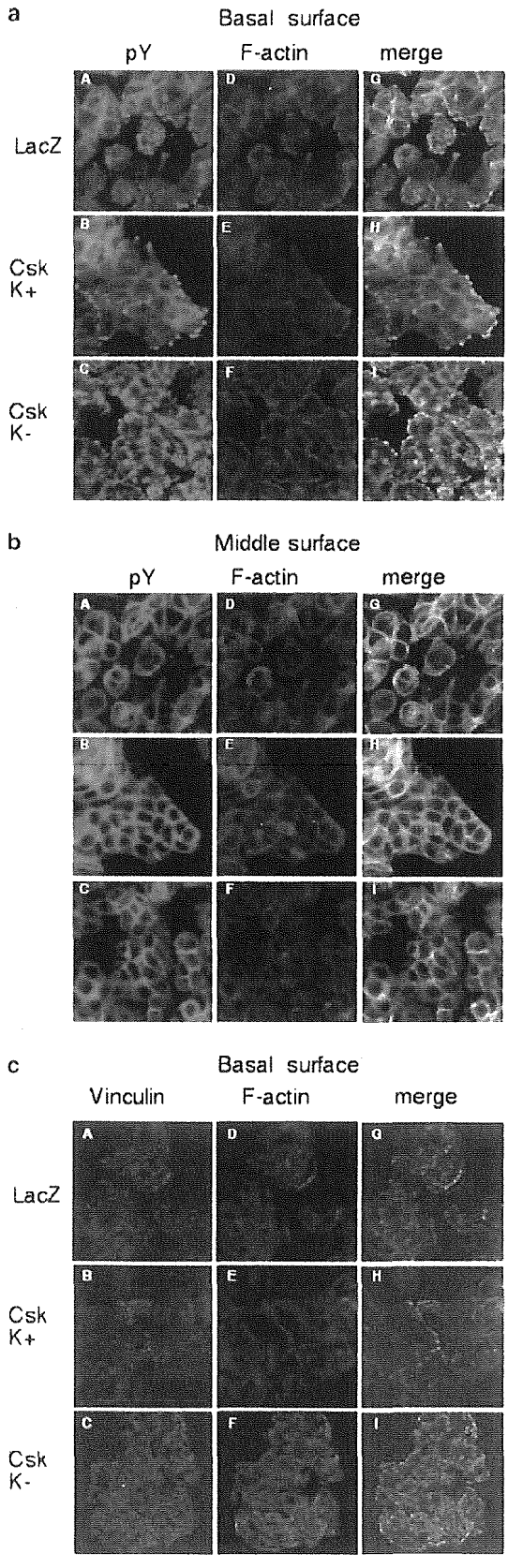

even in the scattered cells. Tyrosine phosphorylation of E-cadherin and β-catenin by the activated form of Src has previously been proposed to trigger ubiquitin-mediated degradation (Aberle *et al*., 1997) or endocytosis of the E-cadherin/β-catenin complex (Fujita *et al*., 2002). To test the possible effect of up- or down-regulation of Csk on this mechanism, we determined the protein amounts of the E-cadherin/β-catenin complex and other potential Src targets, α-catenin and p120^{CTN}, and the tyrosine phosphorylation of E-cadherin/β-catenin complex. As shown in Figure 5c, there was no significant change in the amounts of any protein tested in either Csk K+ or Csk K− cells. In addition, only a subtle increase in tyrosine phosphorylation of either E-cadherin or β-catenin was detected even in Csk K− cells. These findings demonstrate that there is no apparent change in E-cadherin/β-catenin related cell–cell contact machinery and that the activity of endogenous SFK is not sufficient for the phosphorylation-mediated endocytosis of the E-cadherin/β-catenin complex. This raises the possibility that cell–cell contact mediated by E-cadherin/β-catenin is deregulated by SFK through an indirect pathway. Supporting this possibility, we observed that there was a dramatic mobilization of F-actin from cell–cell contacts to focal contacts by modulating SFK function (Figure 4a). Thus, it seems likely that rearrangement of actin cytoskeleton induced by SFK activation causes a loss of actin-support for the E-cadherin/β-catenin complex, thereby destabilizing clustering of the complex that allows high-affinity interaction.

Csk could control metastatic potential of cancer cells through regulating integrin-SFK-mediated cell adhesion signaling

In summary, we here showed that upregulation of Csk in human epithelial cancer cells suppresses the activation of SFK upon cell adhesion, thereby allowing cell–cell contacts mediated by E-cadherin leading to epithelial-like phenotype, and conversely that downregulation of Csk greatly enhances integrin-mediated activation of SFK, which accompanies increased phosphorylation of cell adhesion proteins, cell scattering with mesenchymal-like phenotype, increased number of focal contacts, reorganization of cytoskeletal support, enhanced cell adhesion and migration and *in vitro* invasiveness. These observations suggest that Csk plays a key role in the regulation of the activity status of SFK that influences epithelial–mesenchymal transition (EMT) and the metastatic potential of epithelial cancer cells. Src has been implicated in the regulation of EMT (Frame, 2002), and

Figure 4 Effect of Csk overexpression on the formation of focal contacts and arrangements of actin cytoskeleton. HT 29 cells were infected with adenovirus as described above, and stained with 4G10 (**a** and **b**) or anti-vinculin antibody (**c**) followed by detection with FITC-conjugated anti-mouse IgG. F-actin was stained by rhodamine-phalloidine. Immunofluorescence confocal microscopy pictures were taken at the cell basement in contact with the substratum (basal surface) or 2 μm above the basal surface (middle surface)

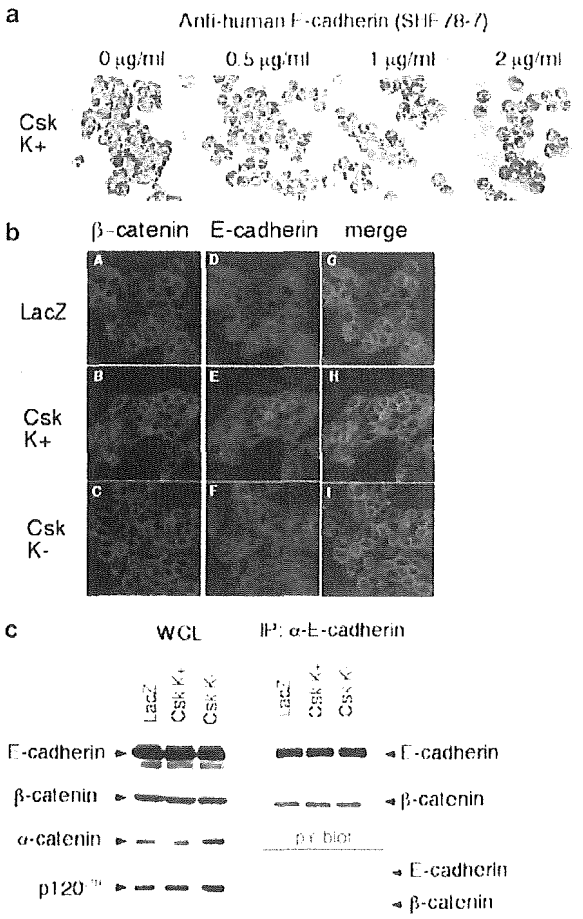

Figure 5 Effect of Csk overexpression on localization, expression and phosphorylation of E-cadherin/β-catenin complex. (**a**) Inhibition of cell–cell contacts by anti-E-cadherin antibody. HT29 cells were infected with adenovirus carrying Csk K+ in the presence of indicated concentrations of anti-E-cadherin antibody (SHE78-7). After 48 h, cells were observed under phase-contrast microscopy. (**b**) HT29 cells infected with indicated adenoviruses were stained with anti-β-catenin and anti-E-cadherin antibodies followed by Cy3-conjugated and FITC-conjugated secondary antibodies, respectively. Pictures were taken at the middle surface (2 μm above the basal surface). (**c**) Total cell lysates from HT29 cells, treated as described above, were subjected to Western blotting using antibodies against E-cadherin, β-catenin, α-catenin and p120^{CTN} (left panels). For analysis of tyrosine phosphorylation of E-cadherin/β-catenin complex, the complex was immunoprecipitated with anti-E-cadherin antibody and then probed with anti-E-cadherin, anti-β-catenin or 4G10 (right panels)

requirement of integrin signaling in such process has also been reported (Avizienyte *et al*., 2002). However, most of the studies on the function of Src were performed using v-Src or active form of Src having a mutation at the C-terminal regulatory site. A natural Src mutant, Src531 (Irby *et al*., 1999), has also been used, but this mutation does not seem to occur frequently (Daigo *et al*., 1999; Nilbert and Fernebro, 2000; Wang *et al*., 2000; Laghi *et al*., 2001). These molecules cannot be regulated by Csk and show constitutively high activity. Using these activated forms of Src, it has been proposed that deregulation of cell–cell contacts mediated by E-cadherin is due to SFK-induced phosphorylation of E-cadherin/β-catenin complex leading to endocytosis and degradation of the complex (Aberle *et al*., 1997; Fujita *et al*., 2002). In the present study, however, significant phosphorylation and degradation of E-cadherin/β-catenin complex were not observed, suggesting that endogenous SFK activity is not sufficient or too weak to be responsible for such degradation pathway of E-cadherin/β-catenin complex in some cancer cells. Nonetheless, the E-cadherin-mediated cell–cell contacts were destabilized by the activation of SFK. In this study, we proposed the possibility that endogenous SFK dominantly regulates integrin-mediated cell adhesion in any cell type. Thus, it would be possible that deregulation of cell–cell contacts may result from secondary events such as reorganization of actin cytoskeleton, although more detailed analysis for the molecular mechanism underlying these events should be necessary. As already mentioned, other members of SFK, Yes and Lck, are upregulated in some colon cancers (Veillette *et al*., 1987; Boardman and Karnes, 1995). In HCT15 and HT29 cells used in this study, a variety of SFK members, that is, Src, Yes, Fyn, Lyn and Lck, are expressed and some are indeed activated. In addition, multiple members of SFK, including Src, Fyn, Hck and Fgr, have been shown to be involved in integrin signaling that is critical for the regulation of metastasis (Suen *et al*., 1999; Cary *et al*., 2002). Taking these observations together with the fact that SFK has redundant function, it is likely that deregulation of the balance between multiple SFKs and Csk achieved by elevated expression of SFKs, down-regulation of Csk or both could influence the metastatic potential of some cancer cells through primarily regulating integrin-mediated cell adhesion signaling.

We showed here that upregulation of Csk function could attenuate the metastatic potential of human colon cancer cells. Our results may provide an insight for therapy in cancer metastasis. Inhibitors of SFK, such as PP2, are known to have harmful side effects. Instead, Csk might be a more selective target for cancer therapy. Gene transfer of Csk has already been undertaken and it successfully suppressed the metastatic activity of colon cancer cells (Nakagawa *et al*., 2000). Since the structure of Csk is now available (Ogawa *et al*., 2002), a specific compound that binds to the SH2 domain to activate Csk may be designed; alternatively, a drug that can activate the expression of Csk may be useful.

Materials and methods

Cell culture and reagents

Colon adenocarcinoma cell lines HCC2998, HCT15 and HT29, and a gastric cancer cell line MKN22 were obtained from the Cancer Chemotherapy Center, Japanese Foundation for Cancer Research (Tokyo, Japan). Cells were cultured in RPMI 1640 medium (Life Technologies, Inc., Grand Island, NY, USA) supplemented with 10% heat-inactivated fetal bovine serum, 2 mmol/l glutamine, 50 μg/ml penicillin and 50 μg/ml streptomycin. Cells were maintained at 37°C and 5%

CO_2 in a humidified atmosphere. Cells were cultured in collagen I, laminin or poly- D-lysine-coated dishes (BD Biocoat, CA, USA) and used for experiments after reaching 80% of confluence. PP2 was purchased from Calbiochem (La Jolla, CA, USA). Stock solutions of this compound were prepared in 100% DMSO (Sigma, St Louis, MO, USA) and stored at −70°C. Coating was performed with 50 μg/ml collagen I on Lab-Tech plastic chamber (Nalge Nunc International, Rochester, NY, USA) (strong coat). Ax1CAT-lacZ, Ax1CATcsk K+ and Ax1CATcsk K− adenovirus were obtained as described elsewhere (Takayama *et al*., 1999).

Western blotting and immunoprecipitation

Cells were washed, and lysed in ODG buffer (50 mM Tris-Hcl, pH 8.0, 1 mM EDTA, 0.25 M NaCl, 20 mM NaF, 1 mM Na_3VO_4, 1% Nonidet P-40, 2% octyl-D-glucoside, 5 mM β-mercapto-ethanol, 10 μg/ml aprotinin, 10 μg/ml leupeptin, 1 mM PMSF, 5% glycerol). Proteins separated by SDS–PAGE were then transferred onto a nitrocellulose membrane (Schleicher & Schuell, NH, USA). Subsequently, the membrane was treated with blocking buffer (Tris-buffered saline containing 0.1% Tween 20 (Tween-TBS)) for 2 h at room temperature. The blocked membrane was probed with primary antibodies and further incubated with a secondary antibody conjugated with horseradish peroxidase. The immunoreactivity was visualized with an enhanced chemiluminescence system (Perkin-Elmer Life Sciences, MA, USA). Primary antibodies used were antiphosphotyrosine (clone 4G10), anti-Yes, anti-FAK (clone 77), anti-E-cadherin (clone 36), anti-$p120^{CTN}$ (clone 98) and anti-α catenin (clone 5) from Transduction Laboratories (KY, USA); anti-v-Src (clone Mab 327) from Calbiochem (San Diego, CA, USA); anti-Csk (clone c-20), anti-Fyn (clone FYN3), anti-Lyn (clone 44), anti-Lck (clone 2102) and anti-β-catenin (clone H-102) from Santa Cruz Laboratories (CA, USA); anti-Src pY418 and pY529, and FAK pY397 from Biosource Laboratories (CA, USA). Horseradish peroxidase-conjugated anti-mouse IgG (Zymed Laboratories Inc., CA, USA) and horseradish peroxidase-conjugated anti-rabbit IgG (Zymed Laboratories Inc., CA, USA) were used as secondary antibodies. For immunoprecipitation, precleared lysate (500 μg protein) was incubated with indicated antibodies and Protein G-Sepharose (Amersham Pharmacia, Buckinghamshire, UK) for 2 h at 4°C. The immunoprecipitate was washed with ODG buffer and analysed by Western blotting.

Cell motility and invasion assay

HT29 cells infected with adenovirus for 24 h were replated on 35 mm glass-bottom microwell dishes (IWAKI) coated with 50 μg/ml collagen I. Cell movements were monitored using Olympus IX71 microscope for 24 h. Images were collected with Cool SNAP HQ CCD camera (Roper) at 6 min intervals, digitized and stored as image stacks using MetaMorph 5.0 software (Universal Imaging). Movements of individual cells were analysed using Move-tr/2D software (Library, Tokyo). For *in vitro* invasion assay, cells (1.0×10^5) were seeded into matrigel invasion chambers (BD Biocoat, CA, USA) in serum-free RPMI media (500 μl), with full RPMI media (700 μl) in the well below. Cells were allowed to grow for 48 h, after which the layer of cells in the chamber was carefully scraped off and cells adhering to the membrane beneath the chambers were stained with crystal violet and counted.

Immunofluorescence staining and confocal microscopy

HT29 cells were infected with adenovirus carrying lacZ (control), Csk K+ or Csk K− on collagen-coated glass coverslips for 2 days. After fixation with 3.7% formaldehyde in PBS for 10 min, cells were incubated with anti-E cadherin, anti-β-catenin, anti-vinculin or antiphosphotyrosine (4G10) antibody in Tris-buffered saline containing 0.1% Tween 20; and further incubated with fluorescein isothiocyanate (FITC)-conjugated anti-mouse IgG antibody (Amersham Pharmacia Biotech, Buckinghamshire, UK) or Cy3-conjugated anti-rabbit IgG antibody (Chemichon, CA, USA). Rhodamine-phalloidin (Eugene, OR, USA) was used to stain F-actin. The stained cells were observed by immunofluorescence microscopy and/or confocal microscopy using an LSM510 (Zeiss, Germany). For inhibition assay of cell–cell contacts, HT29 cells were infected with adenovirus carrying Csk K+ in the presence of indicated concentrations of anti-human E-cadherin antibody (SHE78-7, TAKARA, Japan) for 48 h.

Acknowledgements
We thank Wouter Hazenbos for helpful discussions. This work was supported by the Research Foundation of Japan Society for the Promotion of Science and by a grant-in-aid for Scientific Research of Priority Areas, Cancer, from Ministry of Education, Culture, Sports, Science and Technology. WR-C was supported by a fellowship from the Japanese Society for the Promotion of Science.

References

Aberle H, Bauer A, Stappert J, Kispert A and Kemler R. (1997). *EMBO J.*, **16**, 3797–3804.
Avizienyte E, Wyke AW, Jones RJ, McLean GW, Westhoff MA, Brunton VG and Frame MC. (2002). *Nat. Cell Biol.*, **4**, 632–638.
Boardman LA and Karnes Jr WE. (1995). *Gastroenterology*, **108**, 291–294.
Bolen JB, Veillette A, Schwartz AM, DeSeau V and Rosen N. (1987). *Proc. Natl. Acad. Sci. USA*, **84**, 2251–2255.
Cartwright CA, Coad CA and Egbert BM. (1994). *J. Clin. Invest.*, **93**, 509–515.
Cartwright CA, Kamps MP, Meisler AI, Pipas JM and Eckhart W. (1989). *J. Clin. Invest.*, **83**, 2025–2033.
Cary LA, Klinghoffer RA, Sachsenmaier C and Cooper JA. (2002). *Mol. Cell. Biol.*, **22**, 2427–2440.
Daigo Y, Furukawa Y, Kawasoe T, Ishiguro H, Fujita M, Sugai S, Nakamori S, Liefers GJ, Tollenaar RA, van de Velde CJ and Nakamura Y. (1999). *Cancer Res.*, **59**, 4222–4224.
Dan S, Tsunoda T, Kitahara O, Yanagawa R, Zembutsu H, Katagiri T, Yamazaki K, Nakamura Y and Yamori T. (2002). *Cancer Res.*, **62**, 1139–1147.
Frame MC. (2002). *Biochim. Biophys. Acta*, **1602**, 114–130.
Fujita Y, Krause G, Scheffner M, Zechner D, Leddy HE, Behrens J, Sommer T and Birchmeier W. (2002). *Nat. Cell Biol.*, **4**, 222–231.
Hauck CR, Hsia DA and Schlaepfer DD. (2002). *IUBMB Life*, **53**, 115–119.
Hyafil F, Morello D, Babinet C and Jacob F. (1980). *Cell*, **21**, 927–934.
Imamoto A and Soriano P. (1993). *Cell*, **73**, 1117–1124.
Irby RB, Mao W, Coppola D, Kang J, Loubeau JM, Trudeau W, Karl R, Fujita DJ, Jove R and Yeatman TJ. (1999). *Nat. Genet.*, **21**, 187–190.

Irby RB and Yeatman TJ. (2002). *Cancer Res.*, **62,** 2669–2674.
Kobayashi M, Nagata S, Iwasaki T, Yanagihara K, Saitoh I, Karouji Y, Ihara S and Fukui Y. (1999). *Proc. Natl. Acad. Sci. USA*, **96,** 4874–4879.
Laghi L, Bianchi P, Orbetegli O, Gennari L, Roncalli M and Malesci A. (2001). *Br. J. Cancer*, **84,** 196–198.
Nada S, Okada M, MacAuley A, Cooper JA and Nakagawa H. (1991). *Nature*, **351,** 69–72.
Nada S, Yagi T, Takeda H, Tokunaga T, Nakagawa H, Ikawa Y, Okada M and Aizawa S. (1993). *Cell*, **73,** 1125–1135.
Nakagawa T, Tanaka S, Suzuki H, Takayanagi H, Miyazaki T, Nakamura K and Tsuruo T. (2000). *Int. J. Cancer*, **88,** 384–391.
Nam JS, Ino Y, Sakamoto M and Hirohashi S. (2002). *Clin. Cancer Res.*, **8,** 2430–2436.
Nilbert M and Fernebro E. (2000). *Cancer Genet. Cytogenet.*, **121,** 94–95.
Ogawa A, Takayama Y, Sakai H, Chong KT, Takeuchi S, Nakagawa A, Nada S, Okada M and Tsukihara T. (2002). *J. Biol. Chem.*, **277,** 14351–14354.
Okada M and Nakagawa H. (1989). *J. Biol. Chem.*, **264,** 20886–20893.
Okada M, Nada S, Yamanashi Y, Yamamoto T and Nakagawa H. (1991). *J. Biol. Chem.*, **266,** 24249–24252.
Rengifo-Cam W, Masaki T, Shiratori Y, Kato N, Ikenoue T, Okamoto M, Igarashi K, Sano T and Omata M. (2001). *Cancer*, **92,** 61–70.
Rosen N, Bolen JB, Schwartz AM, Cohen P, DeSeau V and Israel MA. (1986). *J. Biol. Chem.*, **261,** 13754–13759.
Sabe H, Knudsen B, Okada M, Nada S, Nakagawa H and Hanafusa H. (1992a). *Proc. Natl. Acad. Sci. USA*, **89,** 2190–2194.
Sabe H, Okada M, Nakagawa H and Hanafusa H. (1992b). *Mol. Cell. Biol.*, **12,** 4706–4713.
Suen PW, Ilic D, Caveggion E, Berton G, Damsky CH and Lowell CA. (1999). *J. Cell Sci.*, **112,** 4067–4078.
Takayama Y, Tanaka S, Nagai K and Okada M. (1999). *J. Biol. Chem.*, **274,** 2291–2297.
Talamonti MS, Roh MS, Curley SA and Gallick GE. (1993). *J. Clin. Invest.*, **91,** 53–60.
Thomas SM and Brugge JS. (1997). *Annu. Rev. Cell Dev. Biol.*, **13,** 513–609.
Veillette A, Foss FM, Sausville EA, Bolen JB and Rosen N. (1987). *Oncogene Res.*, **1,** 357–374.
Wang NM, Yeh KT, Tsai CH, Chen SJ and Chang JG. (2000). *Cancer Lett.*, **150,** 201–204.

[CANCER RESEARCH 63, 8592–8595, December 15, 2003]

Advances in Brief

Activating Transcription Factor 4 Increases the Cisplatin Resistance of Human Cancer Cell Lines

Mizuho Tanabe,[1,3] Hiroto Izumi,[1] Tomoko Ise,[1] Shun Higuchi,[3] Takao Yamori,[4] Kosei Yasumoto,[2] and Kimitoshi Kohno[1]

Departments of [1]Molecular Biology and [2]Surgery II, University of Occupational and Environmental Health, School of Medicine, Kitakyushu, Fukuoka; [3]Division of Pharmaceutical Sciences, Graduate School, Kyushu University, Higashi-ku, Fukuoka; and [4]Division of Molecular Pharmacology, Cancer Chemotherapy Center, Japanese Foundation for Cancer Research, Toshima-ku, Tokyo, Japan

Abstract

Resistance to cisplatin is a major problem in the treatment of solid tumors. To investigate the determinants of cisplatin resistance, we have identified cisplatin-inducible genes by differential display of mRNA. One of the cisplatin-inducible genes was identified as activating transcription factor 4 (ATF4). Northern blot analysis demonstrated that expression of ATF4 is inducible at the transcriptional level. Its expression is also up-regulated in two cisplatin-resistant cell lines. We tested whether cellular levels of ATF4 are responsible for cisplatin sensitivity by examining 11 human lung cancer cell lines. Expression of ATF4 was found to correlate with cisplatin sensitivity ($P = 0.01$). We also evaluated the cisplatin sensitivity of two stable transfectants overexpressing ATF4. Both were less sensitive to cisplatin than the parental cells but equally sensitive to vincristine. Our findings suggest that levels of ATF4 expression could help to predict cisplatin sensitivity.

Introduction

Cisplatin is a potent antitumor agent that has been used successfully to treat various solid tumors (1, 2). However, development of cisplatin resistance is a major obstacle in clinical treatment (1). Resistance is thought to involve several mechanisms, including decreased drug accumulation (3), increased levels of cellular thiols (4), and increased DNA repair activity (5, 6). We have identified previously Y-box binding protein-1 (YB-1), a transcription factor that binds to DNA intrastrand cisplatin cross-links (7). We showed that human cancer cells that overexpressed YB-1 were resistant to cisplatin and that transfection of such cells with a YB-1 antisense expression plasmid increased their drug sensitivity (8). Using differential display, we showed that cisplatin induced one proton pump subunit gene and that several pump subunit genes were up-regulated in cisplatin-resistant cell lines (9). Cellular pH is also one of the critical parameters affecting cisplatin sensitivity (10).

Cisplatin induces a complex response in cancer cells. Activation of the tumor suppressor gene products p53/p73 by DNA damage signaling can result in cell cycle arrest and apoptosis. Loss of p53 function confers resistance in some human cancer cell lines (11), whereas overexpression of p73 is associated with resistance to cisplatin (12). The relationship between cisplatin sensitivity and damage-induced expression of p53/p73 remains unclear. Several signaling pathways are thought to contribute to resistance to cisplatin. In addition to p53/p73, transcription factors activated in response to cisplatin might be involved in drug sensitivity (11). However, little is known about the expression or activation of such factors. Therefore, the identification of cellular determinants of cisplatin sensitivity could be important for clinical practice. In the current study, we have isolated cisplatin-inducible genes using differential display and report here that activating transcription factor 4 (ATF4) is one of these genes and that it is up-regulated in cisplatin-resistant cell lines. We show also that the expression of ATF4 correlates with cisplatin resistance.

Materials and Methods

Cell Culture. The cisplatin-resistant cell line KB/CP4 derived from human KB epidermoid cancer cells and the cisplatin-resistant cell line P/CDP6 derived from PC3 prostate cancer cells have been described previously (9). They were cultured in Eagle's MEM (Nissui Seiyaku, Tokyo, Japan) containing 10% fetal bovine serum. KB/CP4 and P/CDP6 were found to be 63- and 23-fold, respectively, more resistant to cisplatin than their parental cells (3, 13). Eleven lung cancer cell lines were cultured as described (14).

Drugs and Antibodies. Cisplatin, vincristine, and etoposide were from Sigma (St. Louis, MO). An anticyclic adenosine monophosphate-responsive element binding-2 antibody to ATF4 was purchased from Santa Cruz Biotechnology (Santa Cruz, CA), and anti-high mobility group 1 (HMG1), anti-thioredoxin (TRX) -1, and anti-YB-1 antibodies were made as described previously (8, 15, 16).

Differential Display. Total RNA was isolated by the method described previously (17). For differential display, we used a differential display kit from Takara Shuzo (Kyoto, Japan). In brief, reverse transcription was carried out using 9 anchored primers, and 24 10-mer primers were used with the appropriate anchored primers. Untreated and cisplatin-treated KB cells were analyzed simultaneously. Gels were dried and autoradiographed for 1–2 days, and DNA fragments were eluted from the gels by boiling and were reamplified by PCR. cDNA fragments were then cloned into pGEM-Teasy (Promega, Madison, WI) and sequenced.

Northern Blot Analysis. Northern blot analysis was carried out on total RNA extracted from the indicated cells. The ATF4 cDNA fragment was labeled with random primers using the Megaprime DNA labeling kit (Amersham, Aylesbury, United Kingdom) and hybridized at 42°C in Ultra-hyb solution (Ambion, Austin, TX). Signal intensity was quantified using a bio-imaging analyzer (BAS 2000; Fujix, Tokyo, Japan).

Western Blot Analysis. Whole cell extracts were analyzed by 10% SDS-PAGE. Protein fractions were transferred onto polyvinylidene fluoride membranes, and the membranes were incubated with antibodies against ATF4 (1:1000), YB-1 (1:5000), HMG1 (1:2500), and TRX1 (1:2000) for 1 h at 25°C and visualized by chemiluminescence with the enhanced chemiluminescence protocol (Amersham Biosciences, Piscataway, NJ).

Cytotoxicity Assays. Cells were seeded in 96-well tissue culture plates at 2×10^3 cells/well, and drugs were added the following day. After 72 h, surviving cells were assayed with TetraColar ONE (Seikagaku Corporation, Tokyo, Japan) for 2 h at 37°C according to the protocol provided, and absorbance was measured at 450 nm.

Statistical Analysis. Cellular levels of ATF4 were assessed numerically with the NIH image system. The Pearson correlation was used for statistical analysis, and significance was set at the 5% level.

Construction of an Expression Plasmid. A plasmid containing a full-length cDNA fragment of human ATF4 was generated by reverse transcrip-

Received 6/30/03; revised 9/30/03; accepted 10/16/03.

Grant Support: Mext. Kakenhi (13218132) and AstraZeneca Research Grant 2002.

The costs of publication of this article were defrayed in part by the payment of page charges. This article must therefore be hereby marked *advertisement* in accordance with 18 U.S.C. Section 1734 solely to indicate this fact.

Requests for reprints: Kimitoshi Kohno, Department of Molecular Biology, University of Occupational and Environmental Health, School of Medicine, Yahatanishi-ku, Kitakyushu, Fukuoka 807-8555, Japan. Phone: 81-93-691-7423; Fax: 81-93-692-2766; E-mail: k-kohno@med.uoeh-u.ac.jp.

tion-PCR using total RNA from KB cells, and the cDNA was cloned into pGEM-Teasy (Promega). To construct a mammalian expression plasmid, the *Eco*RI fragment of ATF4 cDNA was cloned into pcDNA3 (Invitrogen, Carlsbad, CA). The following oligonucleotides were used to construct the ATF4 cDNA (GenBank accession no. NM001675): 5′-ATGACCGAAATGAGCTTCCTGAGC-3′ and 5′-CTAGGGGACCCTTTTCTTCCCCC-3′.

Stable Transfection. A549 cells were seeded into 12-well tissue culture plates at a concentration of 5×10^4. The following day they were transfected with 0.3 μg of either pcDNA3 or the pcDNA3-ATF4 expression plasmid using 6 μl of effectene transfection reagent (Qiagen, Hilden, Germany) according to the manufacturer's instructions. After 24 h, the cells were transferred to fresh medium in a new plate. The following day they were challenged with selection medium containing 300 μg/ml of geneticin (Life Technologies, Inc., Rockville, MD) and incubated for 3–4 weeks. Several transfectants that overexpressed the *ATF4* gene were selected. These transfectants, referred to as A549-ATF4, were maintained in the presence of 300 μg/ml of geneticin.

Results and Discussion

ATF4 Expression Is Cisplatin-Inducible and Up-Regulated in Cisplatin-Resistant Cell Lines. To isolate cisplatin-inducible genes, we performed differential display on total RNA from paired untreated and cisplatin-treated KB cells (9). Sequence analysis of the cisplatin-inducible cDNA clones showed that one was identical to the *ATF4/CREB2* gene, and Northern blot analysis demonstrated that this ATF4 mRNA was induced ~5-fold by cisplatin treatment after 24 h (Fig. 1*A*). ATF4 (M_r 39,000) protein levels also increased (Fig. 1*B*). In addition, ATF4 mRNA was up-regulated >2-fold in two independently isolated cisplatin-resistant cell lines, and ATF4 protein was ~3- to 5-fold higher (Fig. 1, *C* and *D*). These data suggest that ATF4 is involved in cisplatin resistance.

ATF4 Expression and Cisplatin Sensitivity in 11 Lung Cancer Cell Lines. We analyzed ATF4 expression and cisplatin sensitivity in 11 human lung cancer cell lines. All of the cell lines have a similar growth rate except A529L, which is shown in Fig. 2*A* by the doubling time. Western blot analysis revealed various levels of ATF4 expression (Fig. 2*A*): A549 and B203L cells had the strongest expression, and PC1 cells had the weakest. To determine whether ATF4 expression was correlated with cisplatin sensitivity, these cell lines were examined for sensitivity to cisplatin, vincristine, and etoposide using cytotoxic assays. There appeared to be a correlation between levels of ATF4 and cisplatin resistance (coefficient of correlation = 0.711; $P = 0.0119$; Fig. 2*B*) but not with resistance to vincristine (coefficient

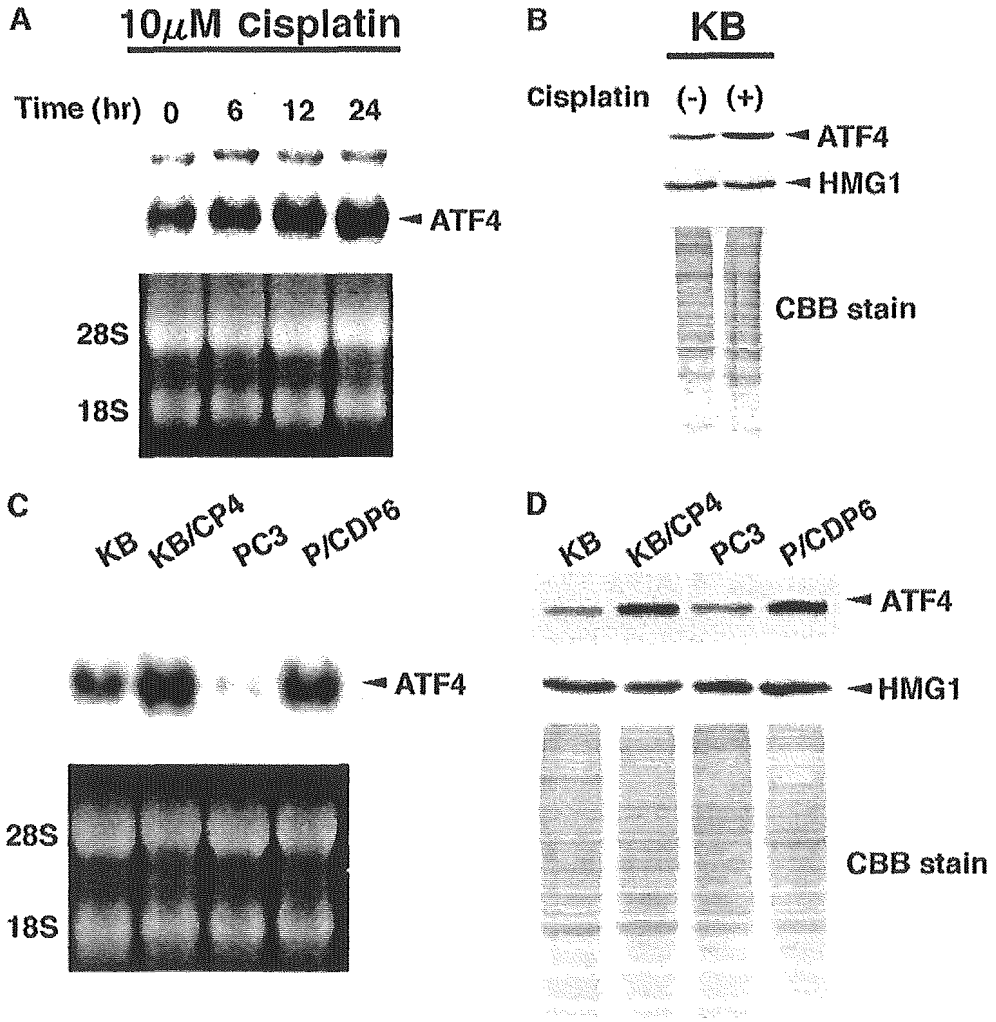

Fig. 1. Expression of activating transcription factor 4 (*ATF4*) in cancer cell lines. *A*, levels of ATF4 mRNA in cisplatin-treated KB cells. KB cells were incubated with cisplatin (10 μM) for the indicated times, and ATF4 mRNA was assayed by Northern blot analysis. Twenty μg of total RNA were loaded per lane. *B*, expression of ATF4 (M_r 39,000) and high mobility group 1 (*HMG1*; M_r 27,000) protein in cisplatin-treated KB cells. KB cells were incubated with cisplatin (10 μM) for 24 h, and ATF4 was assayed by Western blot analysis. Seventy-five μg (*ATF4*) and 25 μg (*HMG1*) of whole cell extract were loaded per lane. *C*, levels of ATF4 mRNA in KB and PC3 cells, and their cisplatin-resistant cells, KB/CP4 and P/CDP6. Fifteen μg of total RNA were loaded per lane. *D*, expression of ATF4 and HMG1 protein in KB and PC3 cells, and their cisplatin-resistant cells, KB/CP4 and P/CDP6. Seventy-five μg (*ATF4*) and 50 μg (*HMG1*) of whole cell extract were loaded per lane. Gel staining is also shown (*bottom*).

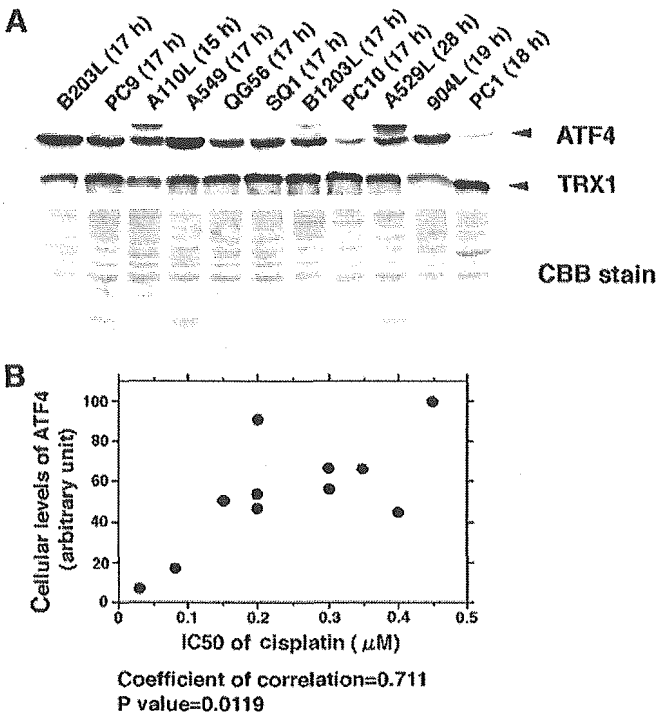

Fig. 2. Association between activating transcription factor 4 (*ATF4*) expression and cisplatin resistance. *A*, levels of ATF4 and thioredoxin-1 (*TRX1*) protein in lung cancer cells. Seventy-five μg (*ATF4*) and 10 μg (*TRX1*) of whole cell extract were loaded per lane and assayed by Western blot analysis. Gel staining is also shown (*bottom*). The doubling time for each cell lines is shown in the *inset*. *B*, correlations between expression level of ATF4 and resistance to cisplatin. Expression levels of ATF4 were determined by NIH image. The maximum expression levels of ATF4 were set to 100, and the IC_{50} of each cell line was calculated from the concentration-response curves for cisplatin.

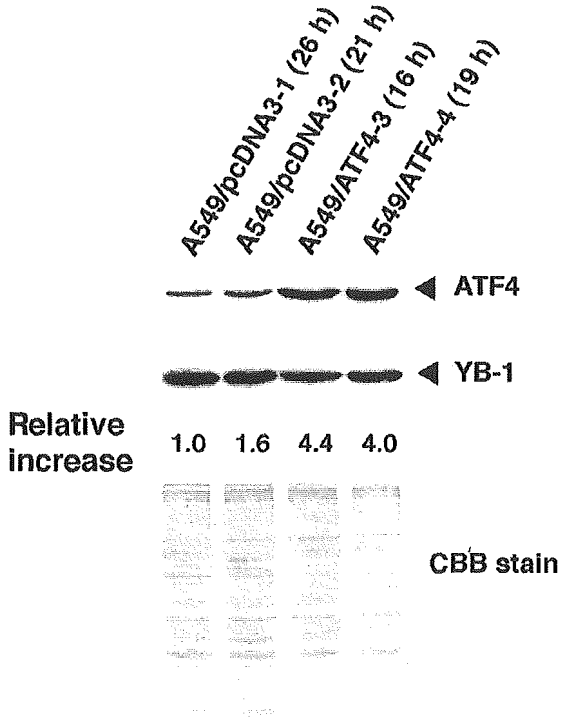

Fig. 3. Western blot analysis of activating transcription factor 4 (*ATF4*) expression in stable transfectants carrying either empty-vector or the pcDNA3-ATF4 expression plasmid. Twenty-five μg of whole cell extract were applied to each lane. Membranes were blotted with antibodies against ATF4 and Y-box binding protein-1 (*YB-1*), and the relative increase of ATF4 content was normalized with YB-1. The doubling time for each cell line is shown in the *inset*.

of correlation = −0.087; $P = 0.8043$) or etoposide (coefficient of correlation = 0.053; $P = 0.8798$). As an additional control, we established that TRX1 expression did not correlate with cisplatin sensitivity (coefficient of correlation = −0.140; $P = 0.6907$). There was no significant correlation between growth rate and sensitivity to cisplatin (data not shown).

Overexpression of ATF4 Increases Resistance to Cisplatin. To determine whether ATF4 is directly involved in cisplatin sensitivity, we established two stable transfectant derivatives of A549 cells. Unfortunately, because of low DNA transfection efficiency, we were unable to establish the stable transfectants from the cell lines with low expression of endogenous ATF4. The expression of endogenous ATF4 is high in A549 cells among 11 lung cancer cell lines. Therefore, it is possible that stable transfectants provide a minor effect against drug sensitivity. The growth rate of these derivatives, A549/ATF4–3 and A549/ATF4–4, was slightly higher than controls transfected with empty vector, and ATF4 expression was increased by 2.5–4.5-fold (Fig. 3). Both derivatives showed increased resistance to cisplatin, with a 3- to 5-fold higher IC_{50} (Fig. 4, *top*). Their sensitivity to vincristine was unaffected (Fig. 4, *bottom*). To our knowledge, this is the first report that ATF4 is DNA-damage inducible and that it is a

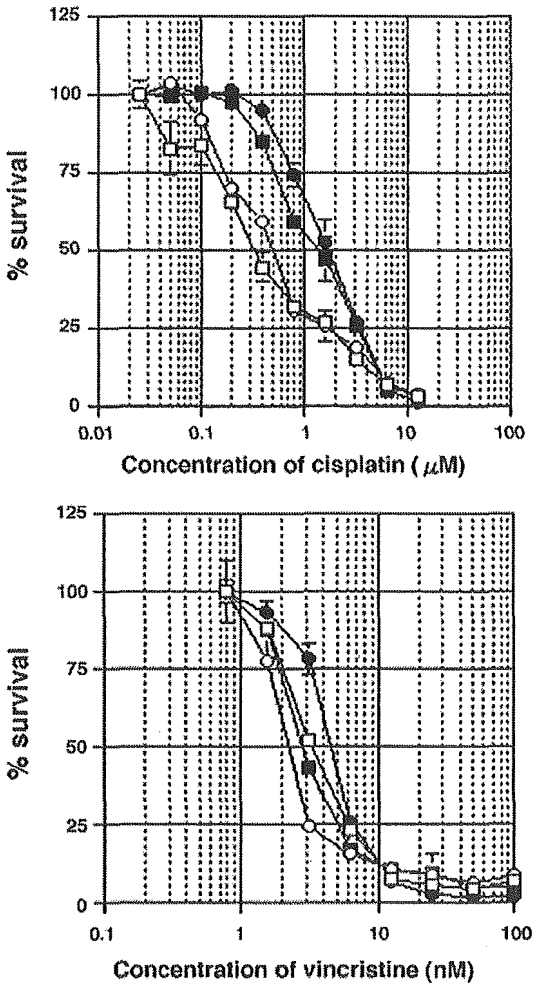

Fig. 4. Concentration-response curve of A549 transfectants to cisplatin and vincristine. Cells were incubated in the absence of drugs for 24 h, and exposed to various concentrations of cisplatin and vincristine for 3 days. Cell number in the absence of drugs corresponds to 100%. Values reported are the mean of at least three independent experiment; *bars*, ± SD. Survival curves of A549 transfectants: A549/pcDNA3–1 (□), A549/pcDNA3–2 (○), A549/ATF4–3 (■), and ATF4–4 (●).

determinant of the cisplatin resistance of human cancer cells. We did not detect any preferential binding of a purified ATF4-GST-fusion protein to cisplatin-modified DNA (data not shown).

ATF4 is a member of the ATF/cyclic adenosine monophosphate-responsive element binding family of transcription factors, and is widely expressed in a variety of tissues and tumor cell lines. It has been shown to form a homodimer *in vitro* that binds to the cyclic adenosine monophosphate response element (18). It has also been shown to interact with nuclear factor-erythroid 1- and 2-related factors, suggesting that it modulates their expression. Nuclear factor-erythroid 1- and 2-related factors are recruited to the antioxidant response element, which plays an important role in the regulation of antioxidant genes (19). We propose that either ATF4 itself or its target genes, Nrf1 and Nrf2, are involved in cisplatin sensitivity. Many genes, including DNA repair genes, contain cyclic adenosine monophosphate response element and/or antioxidant response element in their promoter regions (20). Activating transcription factor 2, another member of the ATF/cyclic adenosine monophosphate-responsive element binding family, is activated by DNA damage and plays a substantial role in drug resistance by promoting DNA repair (21). ATF4-null cells have been shown recently to be impaired in expressing genes involved in glutathione biosynthesis and resistance to oxidative stress (22, 23). Transcription profiling by cDNA arrays has shown that ATF4 is up-regulated in drug-resistant cells that are inducible by genetic suppressor elements (24). Additionally, these data imply that ATF4 expression is involved in drug resistance. Protein kinases that phosphorylate eukaryotic initiation factor 2 are activated by endoplasmic reticulum stress signals and repress translation. These protein kinases selectively increase translation of ATF4, resulting in the induction of target genes (25). Because ATF4 mRNA is increased by cisplatin treatment, it is possible that anticancer agents induce endoplasmic reticulum stress and activate these kinases, increasing ATF4 levels. Further study of the expression of ATF4 target genes may provide insight into the relation between ATF4 expression and cisplatin resistance.

References

1. Cohen, S. M., and Lippard, S. J. Cisplatin: from DNA damage to cancer chemotherapy. Prog. Nucleic Acid Res. Mol. Biol., *67:* 93–130, 2001.
2. Zamble, D. B., and Lippard, S. J. Cisplatin and DNA repair in cancer chemotherapy. Trends Biochem. Sci., *20:* 435–439, 1995.
3. Fujii, R., Mutoh, M., Niwa, K., Yamada, K., Aikou, T., Nakagawa, M., Kuwano, M., and Akiyama, S. Active efflux system for cisplatin in cisplatin-resistant human KB cells. Jpn. J. Cancer Res., *85:* 426–433, 1994.
4. Tew, K. D. Glutathione-associated enzymes in anticancer drug resistance. Cancer Res., *54:* 4313–4320, 1994.
5. Chaney, S. G., and Sancar, A. DNA repair: enzymatic mechanisms and relevance to drug response. J. Natl. Cancer Inst., *88:* 1346–1360, 1996.
6. Husain, A., He, G., Venkatraman, E. S., and Spriggs, D. R. BRCA1 up-regulation is associated with repair-mediated resistance to cis-diamminedichloroplatinum(II). Cancer Res., *58:* 1120–1123, 1998.
7. Ise, T., Nagatani, G., Imamura, T., Kato, K., Takano, H., Nomoto, M., Izumi, H., Ohmori, H., Okamoto, T., Ohga, T., Uchiumi, T., Kuwano, M., and Kohno, K. Transcription factor Y-box binding protein 1 binds preferentially to cisplatin-modified DNA and interacts with proliferating cell nuclear antigen. Cancer Res., *59:* 342–346, 1999.
8. Ohga, T., Koike, K., Ono, M., Makino, Y., Itagaki, Y., Tanimoto, M., Kuwano, M., and Kohno, K. Role of the human Y box-binding protein YB-1 in cellular sensitivity to the DNA-damaging agents cisplatin, mitomycin C, and ultraviolet light. Cancer Res., *56:* 4224–4228, 1996.
9. Murakami, T., Shibuya, I., Ise, T., Chen, Z. S., Akiyama, S., Nakagawa, M., Izumi, H., Nakamura, T., Matsuo, K., Yamada, Y., and Kohno, K. Elevated expression of vacuolar proton pump genes and cellular pH in cisplatin resistance. Int. J. Cancer, *93:* 869–874, 2001.
10. Torigoe, T., Izumi, H., Ishiguchi, H., Uramoto, H., Murakami, T., Ise, T., Yoshida, Y., Tanabe, M., Nomoto, M., Itoh, H., Kohno, K. Enhanced expression of the human vacuolar H+-ATPase c subunit gene (ATP6L) in response to anticancer agents. J. Biol. Chem., *277:* 36534–36543, 2002.
11. Niedner, H., Christen, R., Lin, X., Kondo, A., and Howell, S. B. Identification of genes that mediate sensitivity to cisplatin. Mol. Pharmacol., *60:* 1153–1160, 2001.
12. Vikhanskaya, F., Marchini, S., Marabese, M., Galliera, E., and Broggini, M. P73a overexpression is associated with resistance to treatment with DNA-damaging agents in a human ovarian cancer cell line. Cancer Res., *61:* 935–938, 2001.
13. Nakagawa, M., Nomura, Y., Kohno, K., Ono, M., Mizoguchi, H., Ogata, J., and Kuwano, M. Reduction of drug accumulation in cisplatin-resistant variants of human prostatic cancer PC-3 cell line. J. Urol., *150:* 1970–1973, 1993.
14. Sugaya, M., Takenoyama, M., Osaki, T., Yasuda, M., Nagashima, A., Sugio, K., and Yasumoto, K. Establishment of 15 cancer cell lines from patients with lung cancer and the potential tools for immunotherapy. Chest, *122:* 282–288, 2002.
15. Imamura, T., Izumi, H., Nagatani, G., Ise, T., Nomoto, M., Iwamoto, Y., and Kohno, K. Interaction with p53 enhances binding of cisplatin-modified DNA by high mobility group 1 protein. J. Biol. Chem., *276:* 7534–7540, 2001.
16. Fernando, M. R., Nanri, H., Yoshitake, S., Nagata-Kuno, K., and Minakami, S. Thioredoxin regenerates proteins inactivated by oxidative stress in endothelial cells. Eur. J. Biochem., *209:* 917–922, 1992.
17. Chomczynski, P., and Sacchi, N. Single-step method of RNA isolation by acid guanidinium thiocyanate-phenol-chloroform extraction. Anal. Biochem., *162:* 156–159, 1987.
18. Hai, T., and Hartman, M. G. The molecular biology and nomenclature of the activating transcription factor/cAMP responsive element binding family of transcription factors: activating transcription factor proteins and homeostasis. Gene, *273:* 1–11, 2001.
19. Hayes, J. D., McMahon, M. Molecular basis for the contribution of the antioxidant responsive element to cancer chemoprevention. Cancer Lett., *174:* 103–113, 2001.
20. Mayr, B., and Montminy, M. Transcriptional regulation by the phosphorylation-dependent factor CREB. Nat. Rev. Mol. Cell. Biol., *2:* 599–609, 2001.
21. Hayakawa, J., Depatie, C., Ohmichi, M., and Mercola, D. The activation of NH2-terminal Jun kinase (JNK) by DNA-damaging agents serves to promote drug resistance via phospho-ATF2-dependent enhanced DNA repair. J. Biol. Chem., *23:* 20582–20592, 2003.
22. Harding, H. P., Zhang, Y., Zeng, H., Novoa, I., Lu, P. D., Calfon, M., Sadri, N., Yun, C., Popko, B., Paules, R., Stojdl, D. F., Bell, J. C., Hettmann, T., Leiden, J. M., and Ron, D. An integrated stress response regulates amino acid metabolism and resistance to oxidative stress. Mol. Cell., *11:* 619–633, 2003.
23. Fawcett, T. W., Martindale, J. L., Guyton, K. Z., Hai, T., and Holbrook, N. J. Complexes containing activating transcription factor (ATF)/cAMP-responsive-element-binding protein (CREB) interact with the CCAAT/enhancer-binding protein (C/EBP)-ATF composite site to regulate Gadd153 expression during the stress response. Biochem. J., *339:* 135–141, 1999.
24. Levenson, V. V., Davidovich, I. A., and Roninson, I. B. Pleiotropic resistance to DNA-interactive drugs is associated with increased expression of genes involved in DNA replication, repair, and stress response. Cancer Res., *60:* 5027–5030, 2000.
25. Harding, H. P., Novoa, I., Zhang, Y., Zeng, H., Wek, R., Schapira, M., and Ron, D. Regulated translation initiation controls stress-induced gene expression in mammalian cells. Mol. Cell., *6:* 1099–1108, 2000.

ACADEMIC PRESS

Available online at www.sciencedirect.com

SCIENCE DIRECT®

Biochemical and Biophysical Research Communications 309 (2003) 18–25

BBRC

www.elsevier.com/locate/ybbrc

Rapid discovery and identification of a tissue-specific tumor biomarker from 39 human cancer cell lines using the SELDI ProteinChip platform

Mieko Shiwa,[a] Yumiko Nishimura,[b] Rumi Wakatabe,[a] Ai Fukawa,[a] Hisashi Arikuni,[c] Hiroyuki Ota,[d] Yo Kato,[e] and Takao Yamori[b,*]

[a] *Yokohama Laboratory, Ciphergen Biosystems K.K., Yokohama Business Park East Tower 14F, 134 Godo-cho, Hodogaya-ku, Yokohama, Kanagawa 240-0005, Japan*

[b] *Division of Molecular Pharmacology, Cancer Chemotherapy Center, Japanese Foundation for Cancer Research, 1-37-1 Kami-Ikebukuro, Toshima-ku, Tokyo 170-8455, Japan*

[c] *Yokohama Laboratory, SC Bioscience K.K., Yokohama Business Park Hi-Tech Center 1F, 134 Godo-cho, Hodogaya-ku, Yokohama, Kanagawa 240-0005, Japan*

[d] *Department of Pathology, Cancer Institute, Japanese Foundation for Cancer Research, 1-37-1 Kami-Ikebukuro, Toshima-ku, Tokyo 170-8455, Japan*

[e] *Department of Surgery, Cancer Institute Hospital, Japanese Foundation for Cancer Research, 1-37-1 Kami-Ikebukuro, Toshima-ku, Tokyo 170-8455, Japan*

Received 25 July 2003

Abstract

Useful biomarkers are needed for early detection of cancers. To demonstrate the potential diagnostic usefulness of a new proteomic technology, we performed Expression Difference Mapping analysis on 39 cancer cell lines from 9 different tissues using ProteinChip technology. A protein biomarker candidate of 12 kDa was found in colon cancer cells. We then optimized the purification conditions for this biomarker by utilizing Retentate Chromatography mass spectrometry (RC-MS). The optimized purification conditions developed "on-chip" were directly transferred to conventional chromatography to purify the biomarker, which was identified as prothymosin-α by ProteinChip time-of-flight mass spectrometry (TOF MS) and ProteinChip-Tandem MS systems. The relative expression level of prothymosin-α between colon cancer cells and normal colon mucosal cells was evaluated on the same ProteinChip platform. Prothymosin-α expression in colon cancer cells was clearly higher than in normal colon cells. These results indicate that prothymosin-α could be a potential biomarker for colon cancer, and that the ProteinChip platform could perform the whole process of biomarker discovery from screening to evaluation of the identified marker.

Keywords: ProteinChip; SELDI; Biomarker; Expression Difference Mapping; RC-MS; Colon cancer

New biomarkers associated with a particular disease are in demand to enhance early detection, diagnosis, and prognosis. Several cancer biomarkers have been identified, such as α-fetoprotein (AFP), carcinoembryonic antigen (CEA), and prostate-specific antigen (PSA) [1–4]; however, very few biomarkers are clinically effective. Therefore, the identification of new tumor biomarkers with high positive predictive value or the possibility of being used in conjunction with other biomarkers is needed to expand current clinical capabilities. The ProteinChip platform, based on surface enhanced laser desorption/ionization (SELDI) time-of-flight mass spectrometry [5], has recently been shown to be useful in discovering biomarkers for the diagnosis of bladder [6], prostate [7–10], ovarian [11–13], breast [14–16], liver [17], and other cancers [18–22]. The ProteinChip platform has enabled the approach of Retentate Chromatography mass spectrometry (RC-MS) in which proteins from biological samples are selectivity retained on

* Corresponding author. Fax: +81-3-3918-3716.
E-mail address: yamori@ims.u-tokyo.ac.jp (T. Yamori).

0006-291X/$ - see front matter © 2003 Elsevier Inc. All rights reserved.
doi:10.1016/S0006-291X(03)01520-1

chromatographic surfaces and analyzed directly by mass spectrometry for the purpose of performing differential protein display. This innovative technology has numerous advantages over other methods such as 2D-gel electrophoresis: it has a much higher throughput capability, requires significantly lower amounts of the sample, has subfemtomole range sensitivity, offers higher resolution at low mass ranges, and is easy to use. These advantages could be important for the processing of large sample numbers both to find biomarker candidates and then validate them. In addition to these advantages for biomarker screening, the ProteinChip platform enables rapid purification and identification based on the RC-MS approach [23].

Body fluids, such as serum and urine, are mostly used to investigate and analyze biomarkers. The advantages of body fluid analysis are less pain for patients when obtaining samples and greater accessibility for clinical tests. However, the detection of tissue-specific biomarkers in body fluids requires first that the target protein be secreted, and second, that the biomarker be identified as disease tissue-specific from the multitude of secreted proteins from various cell types and organs. On the other hand, a tissue or cell lysate, when available, can be used to find tumor-specific protein biomarkers more directly from the source.

The object of the present study was identification of a tissue-specific tumor biomarker using cell lysate sample, and demonstration of the capability of ProteinChip technology for biomarker discovery. We performed Expression Difference Mapping analysis on 39 well-characterized human cancer cell lines such as lung, colorectal, gastric, and so on. A specific colon cancer marker protein of 12 kDa was found and identified as prothymosin-α. The study also showed the great potential of ProteinChip technology for the rapid discovery of tumor markers.

Materials and methods

Cell lines and cell culture. A total of 39 human cancer cell lines as a cancer cell panel [24,25] were used for Expression Difference Mapping analysis. The following cell lines were used: lung cancer, NCI-H23, HCI-H226, NCI-H552, NCI-H460, A549, DMS273, and DMS114; colorectal cancer, HCC-2998, KM-12, HT-29, HCT-15, and HCT-116; gastric cancer, St-4, MKN-1, MKN-7, MKN-28, MKN-45, and MKN-74; breast cancer, HBC-4, BSY-1, HBC-5, MCF-7, and MDA-MB-231; ovarian cancer, OVCAR-3, OVCAR-4, OVCAR-5, OVCAR-8, and SK-OV-3; glioma, U251, SF-268, SF-295, SF-539, SNB-75, and SNB-78; renal cancer, RXF-631L and ACHN; melanoma, LOX-IMVI; and prostate cancer, DU-145 and PC-3. All cell lines were cultured in RPMI 1640 supplemented with 5% FBS, penicillin, and streptomycin.

Sample preparation. Cells were harvested after PBS washing from a 100-mm dish and resuspended in 400 μl of lysis buffer (8 M urea, 2% CHAPS, and 1 mM DTT). Whole cell lysates were obtained by sonication on ice followed by centrifugation at 15,000 rpm to remove insoluble debris. Protein concentration was estimated using a Protein Assay Kit (Bio-Rad) and adjusted to 3 mg/ml by adding lysis buffer. All samples were stored at −80 °C. Extracts of normal mucosal cells from colon tissue were used as normal controls and prepared using the same procedure.

Expression Difference Mapping analysis on ProteinChip Arrays. Expression Difference Mapping analysis profiles of the samples were obtained by using strong anion-exchange (SAX2), weak cation-exchange (WCX2), reversed phase (H4), normal phase (NP1), and immobilized affinity capture (IMAC3) ProteinChip Arrays (Ciphergen Biosystems, Fremont, CA, USA). The ProteinChip Arrays were assembled into a deep-well type Bioprocessor assembly (Ciphergen Biosystems). Prior to sample loading, SAX2 and WCX2 arrays were equilibrated with 150 μl of binding buffer (50 mM Tris–HCl, pH 8.5, for SAX2 and 50 mM sodium acetate, pH 4.5, for WCX2), and H4 arrays were pre-washed by 50 μl of binding buffer (10% acetonitrile in PBS). Prior to sample loading, IMAC3 arrays were charged with Ni^{2+} or Cu^{2+} by adding 50 μl of 100 mM $NiSO_4$ or 50 μl of 100 mM $CuSO_4$, respectively. After 5 min incubation, the arrays were quickly rinsed with water to remove unbound metal. For only Cu^{2+} conjugation, the surface was washed with 50 μl of 100 mM sodium acetate, pH 4. The arrays were then equilibrated with 150 μl of binding buffer (PBS). All arrays were then incubated with 50 μl of diluted sample (1 mg/ml) for 20 min on a shaker and washed three times with 150 μl of binding buffer. After rinsing with water, the arrays were removed from the Bioprocessor assembly and air-dried. Each spot of the arrays was circled with a PAP pen (Zymed Laboratories, CA, USA), and two 0.5 μl of saturated sinapinic acid solution (Ciphergen Biosystems) were added in 50% acetonitrile:water containing 0.5% trifluoroacetic acid. The ProteinChip Arrays were analyzed in the ProteinChip Biology System Reader (Model PBS II, Ciphergen Biosystems) and the data were analyzed by ProteinChip Software version 3.0 (Ciphergen Biosystems). All data were normalized by total ion current normalization function following the software instructions. For confirmation of dose-responsibility, various concentrations of trypsin inhibitor (Sigma T-9003) were spiked into whole cell lysate and examined on SAX2 arrays with 20 mM sodium acetate, pH 5.

Purification of biomarker candidate. The purification strategy was determined by ProteinChip Arrays. Whole cell lysates of KM-12 (colon cancer) and NCI-H226 (lung cancer) were diluted 5-fold into 50 mM Tris–HCl, pH 7.5, and loaded onto Q-Sepharose column (Amersham Biosciences). After fractionation by increasing NaCl concentrations, purification progress was monitored using NP1 arrays. The elution of 300 mM NaCl was dialyzed against 20 mM phosphate buffer, pH 7, and then loaded on to Phenyl-Sepharose column (Amersham). After fractionation by decreasing amounts of ammonium sulfate concentration, the purification progress was monitored using H4 arrays. Flow-through fraction of Phenyl-Sepharose column was run on SDS–PAGE for further separation.

Identification of biomarker candidate. Gel pieces containing the target 12 kDa protein were excised. The pieces were incubated sequentially in 50% methanol/10% acetic acid on a shaker at room temperature for 1 h, incubated in 0.1 M ammonium bicarbonate, pH 8.0, on a shaker at room temperature for 1 h, and incubated in 50% acetonitrile, 0.1 M ammonium bicarbonate, pH 8.0, and then 100% acetonitrile (50 μl) for 15 min. After the final acetonitrile incubation, the gel pieces were dried by SpeedVac for 15 min. Bovine pancreatic trypsin (Sequence grade, Roche Diagnostics) in 25 mM ammonium bicarbonate, pH 8.0, or V8 protease (Roche Diagnostics) was added and reacted for 16 h at 37 °C. Reaction solution was applied to the H4 arrays and allow to air-dry. After drying, α-cyano-4-hydroxycinnamic acid solution (0.5 μl; Ciphergen Biosystems) in 50% acetonitrile:water containing 0.1% trifluoroacetic acid was added. To identify the protein, the peptide digests were analyzed both by the ProteinChip Biology System for peptide fingerprint analysis and QSTAR Pulsar i (ABI) equipped with a PCI 1000 ProteinChip Array interface (Ciphergen Biosystems) for sequence tag analysis. Database searches with Mascot and MS-tag were performed.

Results

Dose-responsibility on ProteinChip System

To confirm the quantitative capability of the ProteinChip Biology System, various concentrations of trypsin inhibitor were spiked into cell lysate and analyzed on SAX2 arrays. Fig. 1 shows a representative spectra demonstrating the increase of peak intensity with increasing concentrations of trypsin inhibitor. The dose–response characteristic of the peak intensity with small volume of sample makes the technology particularly valuable for differential display of protein expression in cell lysate samples.

Expression Difference Mapping analysis

Protein profiles of 39 cancer cell lysates were obtained on WCX2, SAX2, IMAC3-Ni^{2+}, IMAC3-Cu^{2+}, NP1, and H4 ProteinChip Arrays. Fig. 2 shows protein profiles of a cell lysate on different types of ProteinChip Array surfaces. Each type of ProteinChip Array surface

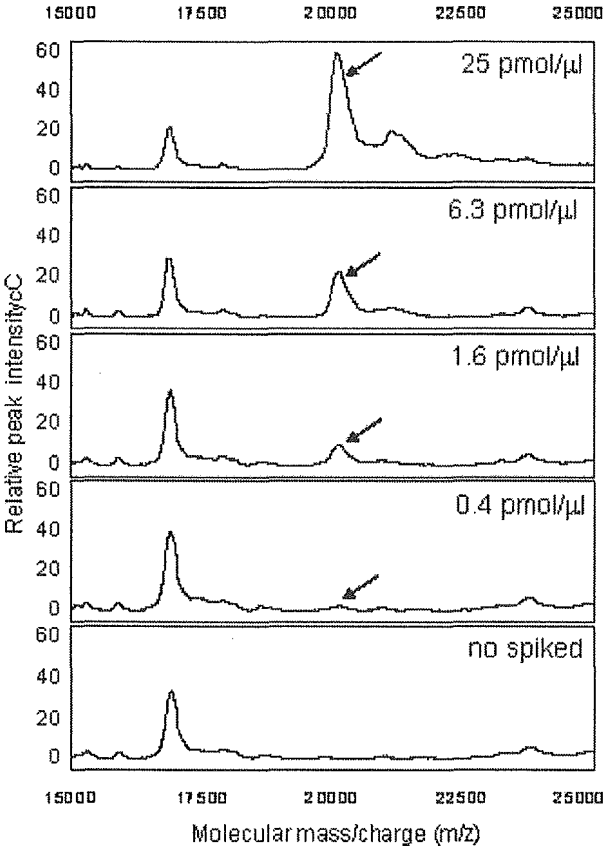

Fig. 1. Dose–response characteristic of the spiked trypsin inhibitor peak into cell lysate. Various concentrations of spiked trypsin inhibitor into cell lysate were analyzed on SAX2 arrays with 20 mM sodium acetate, pH 5. Arrow indicates the trypsin inhibitor peak.

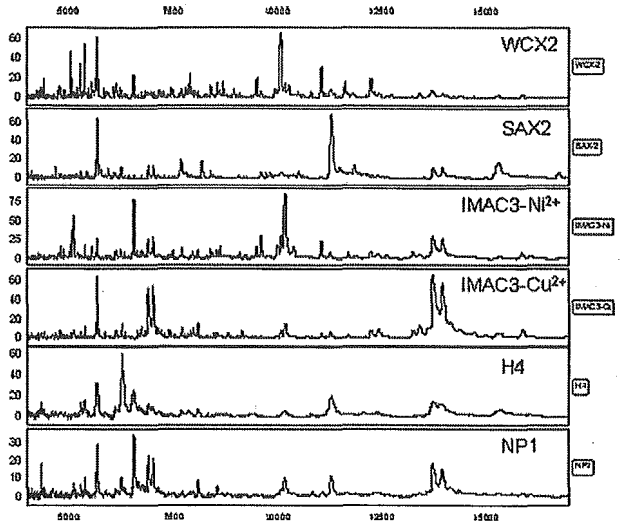

Fig. 2. Protein profiles of a cell lysate on different types of ProteinChip Array surfaces. A cell lysate was analyzed on WCX2, SAX2, IMAC3-Ni^{2+}, IMAC3-Cu^{2+}, H4, and NP1 arrays under the conditions described in the Materials and methods. Profile pattern from 3000 to 20,000 *m/z* is shown.

retained different groups of proteins depending on the array's surface properties. Processing the lysate on each surface resolved between 150 and 200 separate protein peaks in the mass range of 3–100 kDa. Representative spectra of all cell lysates on SAX2 arrays are shown in Fig. 3A. Expression profiles among the samples revealed several protein pattern differences and a 12 kDa protein was found as a highly expressed peak in only colon cancer cell lines. Fig. 3B shows the average peak intensity of this protein in each cancer cell line. The peak intensity of the 12 kDa protein in colon cancer cell lines was remarkably higher than that in other cancer cell lines. The protein peak of 12 kDa was only detected in nuclear extracts fractionated using RIPR buffer (data not shown).

Purification of the 12 kDa marker candidate

Because of the matching chemical properties as chromatographic sorbents, ProteinChip Arrays can be used to develop the purification process. In order to establish a purification procedure for the target 12 kDa protein, we attempted to optimize the adsorption and desorption conditions on arrays. The target protein was only captured on SAX2 arrays, which indicates that strong anion-exchange sorbents were suitable for this purification (data not shown). The optimal pH for retention of the 12 kDa protein was determined to be around 7.5 (Fig. 4A) and buffer pH was fixed for further subsequent experiments. A p*I* value of 3.5–4 was estimated by the data generated on SAX2 arrays (data not shown). Elution of the target protein was accomplished by increasing the concentration of sodium chloride up to

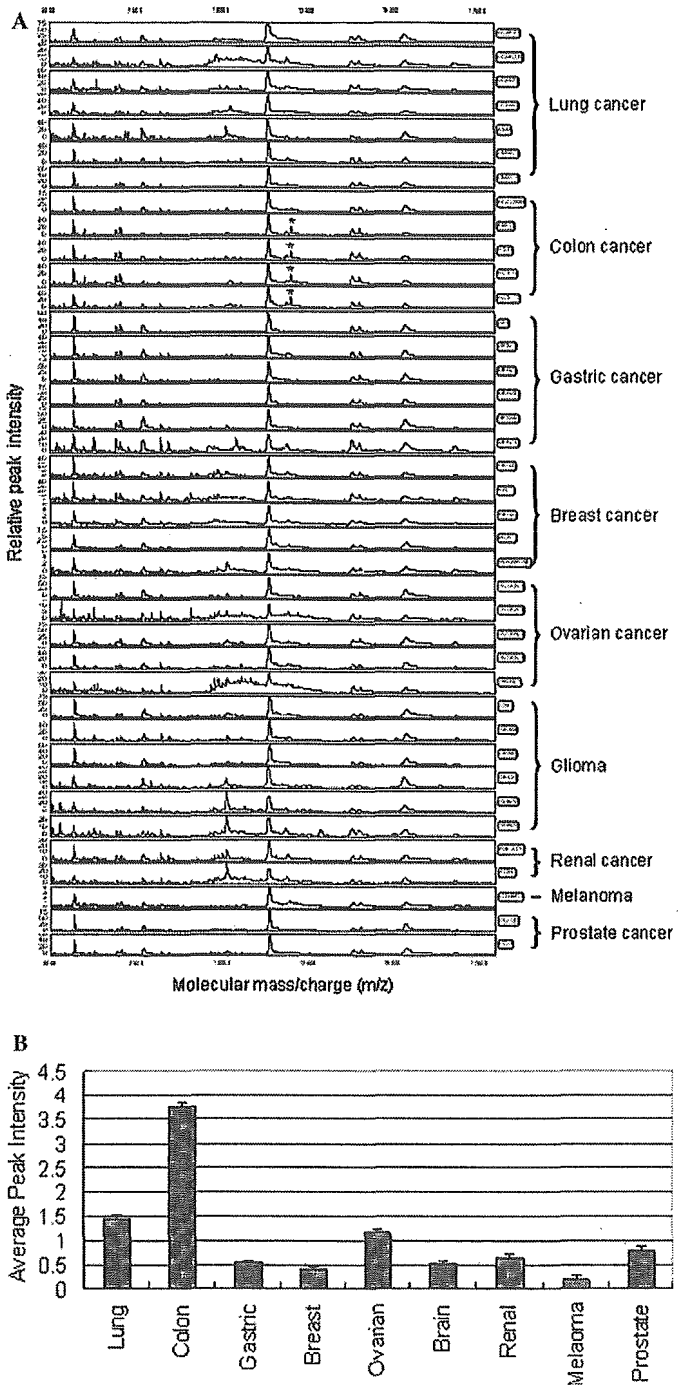

Fig. 3. Marker candidate of colon cancer on expression difference mapping analysis of cancer cell line panel. (A) Protein profiles of cancer cell line panel on SAX2 array. Cell lysates of 39 cancer cell lines were applied to SAX2 array with 50 mM Tris–HCl, pH 8.5. Profile pattern from 5000 to 18,000 *m/z* is shown. Asterisk indicates 12 kDa protein of colon cancer marker candidate. (B) Comparison of the average peak intensity for 12 kDa protein among various tissue cancers.

300 mM in Tris–HCl buffer (Fig. 4B). These optimized purification conditions were directly transferred to small-scale purification using traditional chromatographic methodology incorporating Q-Sepharose beads. Colon cancer cell lysate (KM-12) was diluted with Tris–HCl buffer, pH 7.5, and applied to a Q-Sepharose spin column. After equilibration with the same buffer, elution was performed with a stepwise sodium chloride gradient from 0 to 500 mM. Elution was monitored by profiling on the ProteinChip Biology System. The target protein

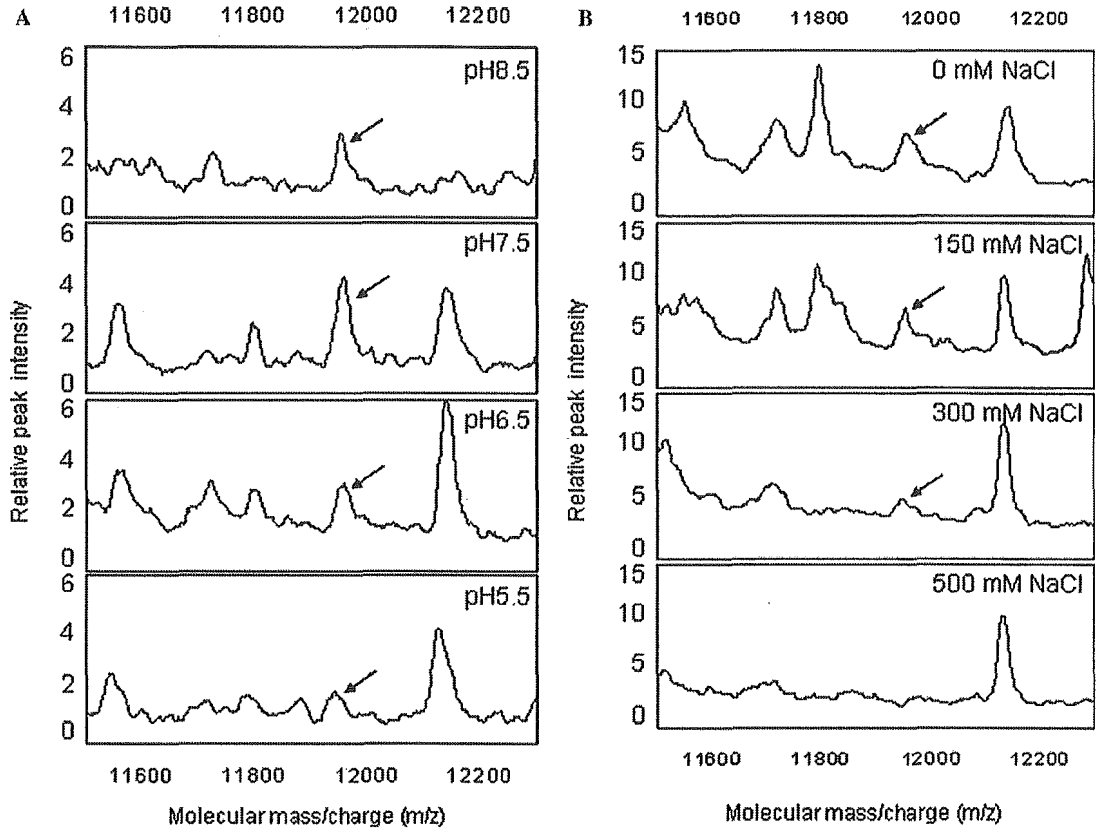

Fig. 4. On-chip optimization of the adsorption and desorption condition. (A) Optimization of buffer pH for retention of 12 kDa marker candidate on SAX2 array. A cell lysate prepared from cell line KM-12 was applied on SAX2 array at the indicated pH. Then, retained proteins on the array were analyzed. Arrow indicates 12 kDa protein peak. The 12 kDa protein was most retained at pH 7.5. (B) Optimization of sodium chloride concentration for desorption of 12 kDa marker candidate on SAX2 array. The cell lysate was dissolved in 50 mM Tris–HCl, pH 7.5, and applied on SAX2 array. The buffer containing the indicated concentration of NaCl eluted the absorbed proteins. Arrow indicates 12 kDa protein peak. It was almost eluted out by 300 mM NaCl.

was eluted in the 300 mM sodium chloride fraction, with the same results as observed via the on-chip optimization analysis (Fig. 5). Then the elution of 300 mM sodium chloride was applied to a Phenyl-Sepharose spin column for further separation from other contaminants, and the target protein was purified in flow-through fraction (data not shown). Lung cancer cell lysate (NCI-H226) was also processed under the same purification procedure as a negative control. The flow-through fractions of the Phenyl-Sepharose spin column were applied to both SDS–PAGE and SELDI analysis for further separation. The results of both analyses were identical, the 12 kDa protein existed in only colon cancer cell lines. The band of 12 kDa in SDS–PAGE analysis was picked up for identification (Fig. 6).

Identification of the 12 kDa marker candidate

In order to further characterize the candidate marker, the protein was digested with trypsin or V8 protease to produce a peptide map for sequence database integration. The proteolysis was performed in gel and the digestion solutions were transferred to the surface of a H4 ProteinChip Array. The set of fragments in the lung cancer cell lysate (NCI-H226) negative control sample was used for subtraction of background from the set of fragments in the target protein in colon cancer cells. Unique peptides in trypsin or V8 proteolysis were entered to Mascot search engine, respectively. Both search results showed that the top matching protein was prothymosin-α. The probability score using the unique fragments of tryptic or V8 proteolysis was 95 ($p < 0.05$) and 81($p < 0.05$); the sequence coverage was 76% and 43%, respectively (data not shown). To confirm this search result, V8 digested 1628.7299 *m/z* fragment was analyzed by collision-induced dissociation (CID)-tandem MS with the ProteinChip Interface. The masses of product ions were applied to the MS-Tag search engine and the fragment of amino acid was confirmed as AENGRDAPANGNAENE of prothymosin-α (data not shown).

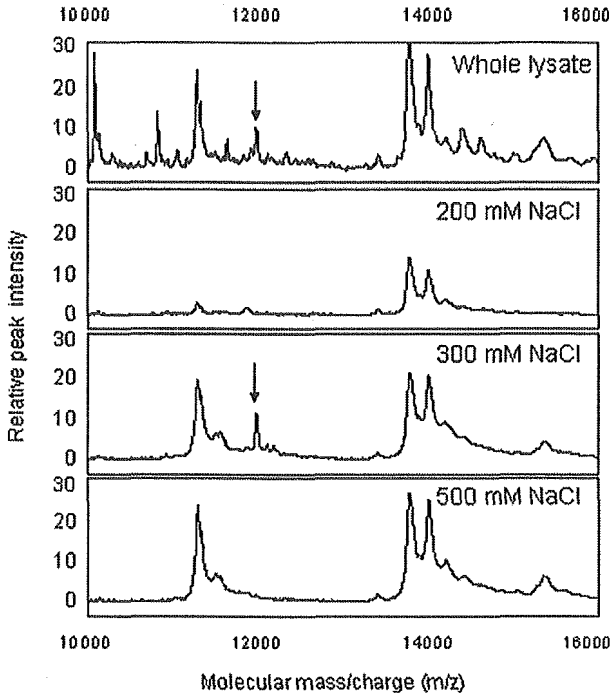

Fig. 5. On-chip monitoring of the elution from Q-spin column purification. The KM-12 cell lysate was applied to Q-spin column with 50 mM Tris–HCl, pH 7.5. The absorbed proteins were eluted by the indicated concentration of NaCl. The eluent was analyzed on SAX2 array with 50 mM Tris–HCl, pH 7.5. Arrow indicates 12 kDa protein peak. The elution of 300 mM NaCl contained the 12 kDa protein in agreement with the desorption condition determined by on-chip optimization (Fig. 4B).

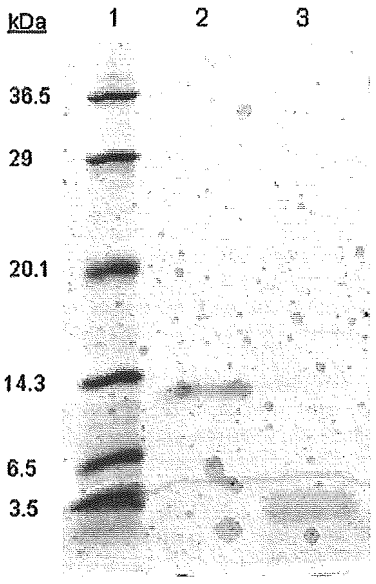

Fig. 6. SDS–PAGE analysis of the purified 12 kDa protein. The flow-through fraction from Phenyl-Sepharose spin column was run on SDS–PAGE gel and stained with Coomassie blue R-250. Lane 1, molecular marker; lane 2, colon cancer cell line (KM-12); and lane 3, lung cancer cell line (NCI-H226).

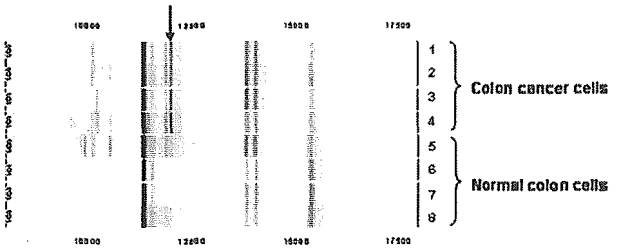

Fig. 7. Comparison of 12 kDa protein expression level between colon cancer cells and normal colon mucosal cells. Both cell lysates from colon cancer cell lines and normal colon mucosal cells were analyzed on SAX2 array with 50 mM Tris–HCl, pH 7.5. Profile pattern from 8000 to 18,000 *m/z* is shown as a gel view image. Arrow indicates 12 kDa marker candidate protein. Lane 1, KM-12; lane 2, HT-29; lane 3, HCT-15; lane 4, HCT-116; lane 5, normal 1; lane 6, normal 2; lane 7, normal 3; and lane 8, normal 4.

Comparison of 12 kDa protein expression level between colon cancer cells and normal colon mucosal cells

In order to confirm whether the 12 kDa biomarker candidate is a colon cancer-specific protein or a colon tissue-specific protein, the protein expression levels of this protein between colon cancer and normal colon mucosal cells were compared. The cell extract profiles were performed on SAX2 arrays at pH 8. Fig. 7 shows that the peak intensity of identified 12 kDa in colon cancer cell lines was clearly higher than that in normal colon mucosal cells.

Discussion

In this study, the capability of the ProteinChip platform for rapid biomarker discovery from crude cell extracts has been demonstrated. The ProteinChip Biology System is ideal for protein biomarker discovery and other protein based applications [23,26–32]. In the present experiments, we compared the profiles of 39 human cancer cell lines using 5 different kinds of array surfaces. We identified and evaluated a protein biomarker candidate for colon cancer. These results indicate that the ProteinChip platform is applicable to perform the whole process of biomarker discovery on the same platform from first marker screening step to evaluation test of the identified marker. Other conventional protein profiling methods, such as 2D-gel electrophoresis, are capable of analyzing several thousand protein features on a gel; however, it is a labor-intensive work, requires large amount of samples, and needs an evaluation assay system using another platform. The ProteinChip platform's powerful advantages save time and amount of samples.

In the purification process, we can directly apply the optimized purification conditions from arrays to

conventional purification using matching chromatography sorbents. Purification of recombinant proteins also has been reported using this approach [23]. The results of our study indicate that the ProteinChip RC-MS approach can be widely adapted to crude biological samples and could be helpful for rapid purification.

In the identification process, we could perform identification by peptide mapping and also CID sequencing using ProteinChip technology. One advantage of using this technology is that the same array can be used first in the ProteinChip Biology System and then the ProteinChip-Tandem MS system. Using both systems makes it possible to cover the entire process from biomarker screening to confirmatory protein identification. ProteinChip-Tandem MS has been demonstrated in the application of on-chip digestion for identification [33] and the on-chip application could be helpful for the micro-scale identification.

Prothymosin-α is an acidic protein (theoretical p*I* 3.5) containing 109–111 amino acids and was first isolated from rat thymus [34]. The estimated value and detected mass by the ProteinChip platform are very close to these theoretical values. Furthermore, prothymosin-α is known as a nuclear protein and our identified peak was also only detected in nuclear extract. These findings strongly support the identification results on both peptide mapping and MSMS analysis.

In colon cancer, CEA and CA19-9 are the two most common clinical tumor markers [35,36]. The positive predictive value of CEA is 40–60% and that of CA19-9 is 30–50%. These two markers are used for evaluating therapeutic effect and monitoring for recurrence in advanced stages; however, these are not useful for screening in earlier stages. It has been reported that mRNA expression of the identified biomarker candidate in this study, prothymosin-α, correlates with that of c-myc in human colon cancer [37]. Also, mRNA expression levels are higher in colon cancer tissue than in normal colon tissues [37]. Although there is no other report concerning protein expression level of prothymosin-α in human colon cancer cells, our results indicate that the expression level of prothymosin-α in cancer cells is clearly higher than in normal colon tissue. Further studies to assess the usefulness of prothymosin-α as a tumor marker of colon cancer in early stage will also be undertaken.

In conclusion, our current investigation demonstrated the ability of the ProteinChip platform for the discovery of biomarkers using crude biological samples. Comparison of cell lysate profiles from cancer cell lines provided an effective approach to screen for potential biomarker candidates. A colon cancer biomarker candidate was rapidly identified and evaluated on the same platform, further demonstrating that the ProteinChip platform is a powerful tool for clinical proteomics.

Acknowledgments

We thank Ms. Kimie Nomura for technical assistance in the preparation of extracts from normal colonic mucosa. We also thank Dr. Lee Lomas and Ms. Sarah Lyn Torres for the very helpful discussions during the preparation of the manuscript.

References

[1] E.P. Mitchell, Role of carcinoembryonic antigen in the management of advanced colorectal cancer, Semin. Oncol. 25 (1998) 12–20.
[2] H.J. Schmoll, J. Beyer, Prognostic factors in metastatic germ cell tumors, Semin. Oncol. 25 (1998) 174–185.
[3] N.L. Bartlett, F.S. Freiha, F.M. Torti, Serum markers in germ cell neoplasms, Hematol. Oncol. Clin. North Am. 5 (1991) 1245–1260.
[4] J.E. Osterling, Prostate specific antigen a critical assessment of the most useful tumor marker for adenocarcinoma of the prostate, J. Urol. 145 (1991) 907–923.
[5] T.W. Hutchens, T.T. Yip, New desorption strategies for the mass spectrometric analysis of macromolecules, Rapid. Commun. Mass Spectrom. 7 (1993) 576–580.
[6] A. Vlahou, P.F. Schellhammer, S. Medrinos, F.I. Kondylis, L. Gong, S. Nasim, G.L. Wright Jr., Development of a novel proteomic approach for the detection of transitional cell carcinoma of the bladder in urine, Am. J. Pathol. 158 (2001) 1491–1501.
[7] E.F. Petricoin, D.K. Ornstein, C.P. Paweletz, A. Ardekani, P.S. Hackett, B.A. Hitt, A. Velassco, C. Trucco, L. Wiegand, K. Wood, C.B. Simone, P.J. Levine, W.M. Linehan, M.R. Emmert-Buck, S.M. Steinberg, E.C. Kohn, L.A. Liotta, Serum proteomic patterns for detection of prostate cancer, J. Natl. Cancer Inst. 94 (2002) 1576–1578.
[8] Y. Qu, B.-L. Adam, Y. Yasui, M.D. Ward, L.H. Cazares, P.F. Schellhammer, Z. Feng, O.J. Semmes, G.L. Wright Jr., Boosted decision tree analysis of surface-enhanced laser desorption/ionization mass spectral serum profiles discriminates prostate cancer from noncancer patients, Clin. Chem. 48 (2002) 1835–1843.
[9] L.H. Cazares, B.-L. Adam, M.D. Ward, S. Nasim, P.F. Schellhammer, O.J. Semmes, G.L. Wright, Normal, benign, preneoplastic, and malignant prostate cells have distinct protein expression profiles resolved by surface enhanced laser desorption/ionization mass spectrometry, Clin. Cancer Res. 8 (2002) 2541–2552.
[10] B. Adam, Y. Qu, J.W. Davis, M.D. Ward, M.A. Clements, L.H. Cazares, O.J. Semmens, P.F. Schellhammer, Y. Yasui, F. Ziding, G. Wright, Serum protein fingerprinting coupled with a pattern-matching algorithm distinguishes prostate cancer from benign prostate hyperplasia and healthy men, Cancer Res. 62 (2002) 3609–3614.
[11] L.A. Liotta, E.F. Petricoin III, A.M. Ardekani, B.A. Hitt, P.J. Levine, V.A. Fusaro, S.M. Steinberg, G.B. Mills, C. Simone, D.A. Fishman, E.C. Kohn, General keynote: proteomic patterns in sera serve as biomarkers of ovarian cancer, Gynecol. Oncol. 88 (2003) S25–S28.
[12] C.A. Bandera, B. Ye, S.C. Mok, New technologies for the identification of markers for early detection of ovarian cancer, Curr. Opin. Obstet. Gynecol. 15 (2003) 51–55.
[13] E.F. Petricoin, A.M. Ardekani, B.A. Hitt, P.J. Levine, V.A. Fusaro, S.M. Steinberg, G.B. Mills, C. Simone, D.A. Fishman, E.C. Kohn, L.A. Liotta, Use of proteomic patterns in serum to identify ovarian cancer, Lancet 359 (2002) 572–577.
[14] J. Li, Z. Zhang, J. Rosenzweig, Y.Y. Wang, D.W. Chan, Proteomics and bioinformatics approached for identification of

serum biomarkers to detecting breast cancer, Clin. Chem. 48 (2002) 1296–1304.
[15] C.P. Paweletz, B. Trock, M. Pennanen, T. Tsangaris, C. Magnant, L.A. Liotta, E.F. Petricoin III, Proteomic patterns of nipple aspirate fluids obtained by SELDI-TOF: potential for new biomarkers to aid in the diagnosis of breast cancer, Dis. Markers 17 (2001) 301–307.
[16] D. Carter, J.F. Douglass, C.D. Cornellison, M.W. Retter, J.C. Johnson, A.A. Bennington, T.P. Fleming, S.G. Reed, R.L. Houghton, D.L. Diamond, T.S. Vedvick, Purification and characterization of the mammaglobin/lipophilin B complex, a promising diagnostic marker for breast cancer, Biochemistry 41 (2002) 6714–6722.
[17] T.C.W. Poon, T.T. Yip, A.T.C. Chan, C. Yip, V. Yip, T.S.K. Mok, C.C.Y. Lee, T.W.T. Leung, S.K.W. Ho, P.J. Johnson, Comprehensive proteomic profiling identifies serum proteomic signatures for detection of hepatocellular carcinoma and its subtypes, Clin. Chem. 49 (2003) 752–760.
[18] T.A. Zhukov, R.A. Johanson, A.B. Cantor, R.A. Clark, M.S. Tockman, Discovery of distinct protein profiles specific for lung tumors and pre-malignant lung lesions by SELDI mass spectrometry, Lung Cancer 40 (2003) 267–279.
[19] T.T. Yip, L. Lomas, Technol. Cancer Res. Treat. 1 (2002) 273–280.
[20] J.D. Wulfkuhle, L.A. Liotta, E.F. Petricoin, Proteomic applications for the early detection of cancer, Nat. Rev. 3 (2003) 267–272.
[21] P.R. Srinivas, M. Verma, Y. Zhao, S. Srivastava, Proteomics for cancer biomarker discovery, Clin. Chem. 48 (2002) 1160–1169.
[22] C. Rosty, L. Christa, S. Kuzdzal, W.M. Baldwin, M.L. Zahurak, F. Carnot, D.W. Chan, M. Canto, K.D. Lillemoe, J.L. Cameron, C.J. Yeo, R.H. Hruban, M. Goggins, Identification of hepatocarcinoma-intestine-pancreas/pancreatitis-associated protein I as a biomarker for pancreatic ductal adenocarcinoma by protein biochip technology, Cancer Res. 62 (2002) 1868–1875.
[23] S.R. Weinberger, E. Boschetti, P. Santambien, V. Brenac, Surface-enhanced laser desorption–ionization retentate chromatography mass spectrometry (SELDI-RC-MS): a new method for rapid development of process chromatography conditions, J. Chromatogr. B 782 (2002) 307–316.
[24] T. Yamori, A. Matsunaga, S. Sato, K. Yamazaki, A. Komi, K. Shizu, I. Mita, H. Edatsugi, Y. Matsuba, K. Takezawa, O. Nakanishi, H. Kohno, Y. Nakajima, H. Komatsu, T. Andoh, T. Tsuruo, Potent antitumor activity of MS-247, a novel DNA minor groove binder, evaluated by in vitro and in vivo human cancer cell line panel, Cancer Res. 59 (1999) 4042–4049.
[25] S. Dan, T. Tsunoda, O. Kitahara, R. Yanagawa, H. Zembutsu, T. Katagiri, K. Yamazaki, Y. Nakamura, T. Yamori, An integrated database of chemosensitivity to 55 anticancer drugs and gene expression profiles of 39 human cancer cell lines, Cancer Res. 62 (2002) 1139–1147.
[26] K. Chapman, The ProteinChip® Biomarker System from Ciphergen Biosystems: a novel proteomics platform for rapid biomarker discovery and validation, Biochem. Soc. Trans. 30 (2002) 82–87.
[27] L. Zhang, W. Yu, T. He, J. Yu, R.E. Caffrey, E.A. Dalmasso, S. Fu, T. Pham, J. Mei, J.J. Ho, W. Zhang, P. Lopez, D.D. Ho, Contribution of human alpha-defensin 1, 2, and 3 to the anti-HIV-1 activity of CD8 antiviral factor, Science 298 (2002) 995–1000.
[28] H. Davies, L. Lomas, B. Austen, Profiling of amyloid beta peptide variants using SELDI ProteinChi® Arrays, BioTechniques 27 (1999) 1258–1262.
[29] T.K. Bane, J.F. LeBlanc, T.D. Lee, A.D. Riggs, DNA affinity capture and protein profiling by SELDI-TOF mass spectrometry: effect of DNA methylation, Nucleic Acids Res. 30 (2002) e69.
[30] P. Melamed, M. Koh, P. Preklathan, L. Bei, C. Hew, Multiple mechanisms for Pitx-1 transactivation of a luteinizing hormone subunit gene, J. Biol. Chem. 277 (2002) 26200–26207.
[31] D. Spencer, L. Robson, D. Purdy, N.R. Whitelegg, N.P. Michael, J. Bhatia, S. Sharma, A. Rees, N.P. Minton, R.H.J. Begent, K. Chester, A strategy for mapping and neutralizing conformational immunogenic sites on protein therapeutics, Proteomics 2 (2002) 271–279.
[32] S.R. Weinberger, R.I. Viner, P. Ho, Tagless extraction-retentate chromatography: a new global protein digestion strategy for monitoring differential protein expression, Electrophoresis 23 (2002) 3182–3192.
[33] G. Reid, B.S. Gan, Y.M. She, W. Ens, S. Weinberger, J.C. Howard, Rapid identification of probiotic lactobacillus biosurfactant proteins by ProteinChip® tandem mass spectrometry tryptic peptide sequencing, Appl. Environ. Microbiol. Feb. (2002) 977–980.
[34] J.Y. Wang, R. Tang, J.M. Chiang, Value of carcinoembryonic antigen in the management of colorectal cancer, Dis. Colon Rectum 37 (1994) 272–277.
[35] A.A. Haritos, G.J. Goodall, B.L. Horecker, Prothymosin alpha: isolation and proaties of the major immunoreactive form of thymosin alpha1 in rat thymus, Proc. Natl. Acad. Sci. USA 81 (1984) 1008–1011.
[36] M. Dies, F.J. Cerdan, M. Pollan, M.L. Maestro, M.D. Ortega, S. Martinez, G. Moreno, J.L. Balibrea, Prognostic significance of reoperative serum CA19.9 assay in patients with colorectal carcinoma, Anticancer Res. 14 (1994) 2819–2825.
[37] M.M. Mori, G.F. Barnard, R.J. Staniunas, M. Jessu, G.D. Steele Jr., L.B. Chen, Prothymosin-α mRNA expression correlates with that of c-*myc* in human colon cancer, Oncogene 8 (1993) 2821–2826.